Multi-Agents Cooperative Target Tracking Under Physical Attacks With Environment-Aware Dynamic Constraints

Zhongjun Hu, Jesse B. Hoagg, *Senior Member, IEEE*, and Xu Jin, *Senior Member, IEEE*

***Abstract*—In this work, we consider a cooperative target tracking problem by multi-agents in a 3D space, under disruptions from multiple physical attackers, where the target and physical attackers are intelligent, that is, they adjust velocities based on relative coordinates with agents and agents' velocities. Due to the presence of physical attackers, some safety and performance constraint requirements cannot be merely constant or time-varying. Specifically, safety constraint requirements on inter-agent distances and performance constraint requirements on formation tracking errors are *environment-aware and dynamic*, which depend on distances between agents and physical attackers. We propose a neural network-based adaptive cooperative control framework for the agents, which incorporates a universal barrier function to handle safety and performance constraints. We show that formation tracking errors are uniformly ultimately bounded, while all safety and performance constraints are met. A comparative simulation study further illustrates the efficacy of the proposed framework.**

***Note to Practitioners*—Cooperative target tracking control for multi-agent systems has gained significant attention due to its real-world applications. In practice, target-tracking tasks are often carried out in complex environments, where multiple physical attackers can fly nearby to disrupt the agents. Moreover, the target and attackers often possess a certain level of intelligence, making the target more difficult to track, complicating an already difficult problem. Thus, most control frameworks in the literature, which assume targets and attackers have constant or time-varying velocities, are not effective to address real-world operational complexities. Additionally, in complex environments, certain constraint requirements need to be environment-aware and dynamic, instead of being mere constants or time-varying. To address these practical challenges, this work proposes a neural network-based adaptive cooperative control framework that integrates a universal barrier function to ensure that all safety and performance constraints are met. Finally, we consider two scenarios in the simulation study to further validate the efficacy of the proposed control framework.**

***Index Terms*—Cooperative target tracking, physical attackers, environment-aware and dynamic constraints, multi-agent systems.**

NOMENCLATURE

N_{a}	Number of attackers ($N_{\mathrm{a}} \geq 2$).
N_{u}	Number of agents ($N_{\mathrm{u}} \geq 2$).
p_i	Velocity of the ith agent ($i \in \{1, \cdots, N_{\mathrm{u}}\}$).
q_{a}	Center of attacker set defined in (37).
$q_{\mathrm{a}k}$	Position of the kth physical attacker ($k \in \{1, \cdots, N_{\mathrm{a}}\}$).
q_{c}	$q_{\mathrm{c}} \triangleq \frac{1}{N_{\mathrm{u}}} \sum_{i=1}^{N_{\mathrm{u}}} q_i$, centriod of all agents.
q_i	Position of the ith agent.
q_{t}	Position of the target.
q_{u}	Center of agent set defined in (35).
$\eta_{\mathrm{au}}, \eta_{\mathrm{t}i}, \eta_{\mathrm{e}ij}$	Transformed error variables defined in (5) and (7), respectively.
Ω_{a}	Constant constraint in control objective (CO1).
$\Omega_{d\mathrm{tc}}$	Environment-aware dynamic performance constraint in control objective (CO4).
$\Omega_{\mathrm{H}ij}, \Omega_{\mathrm{L}ij}$	Environment-aware dynamic safety constraints in control objective (CO3).
$\Omega_{\mathrm{t}i}$	Constant constraint in control objective (CO2).
Π_{tc}	Transformed error variable defined in (9).

I. INTRODUCTION

A. Motivation

COOPERATIVE target tracking by multi-agents has a range of applications, including security management [1], surveillance [2], environment monitoring [3], and beyond. In recent years, there has been a fruitful discussion on this topic, including [4], [5], [6], [7]. In realistic operations of cooperative target tracking, agents can be disrupted by multiple physical attackers, making the target more difficult to track. Such physical attackers not only make the environment significantly more complex, but also render the handling of safety/performance constraints critically important. However, the presence of physical attackers and their effects on the safety/performance constraints have not been studied in the aforementioned literature.

Received 6 February 2025; revised 19 June 2025; accepted 22 August 2025. Date of publication 9 September 2025; date of current version 30 September 2025. This article was recommended for publication by Associate Editor G. Michieletto and Editor A. M. Ghalamzan Esfahani upon evaluation of the reviewers' comments. This work was supported in part by the National Science Foundation under Grant 2131802 and Grant 2336189 and in part the United States Department of Agriculture (USDA) National Institute of Food and Agriculture (NIFA) under Grant 2024-69014-42393. *(Corresponding author: Xu Jin.)*

The authors are with the Department of Mechanical and Aerospace Engineering, University of Kentucky, Lexington, KY 40506 USA (e-mail: ZhongjunHu@uky.edu; jesse.hoagg@uky.edu; xu.jin@uky.edu).

Digital Object Identifier 10.1109/TASE.2025.3607874

To handle state constraints, common methods include control barrier functions (CBFs) [8], [9], [10], [11], barrier functions/barrier Lyapunov functions (BLFs) [12], [13], [14], [15], and model predictive control (MPC) methods [16], [17], [18], [19], [20]. However, these algorithms only deal with constant or time-varying constraint requirements, which are often conservative and cannot respond to environmental factors that are not simply time-varying. In the presence of multiple physical attackers, some constraint requirements need to be dynamic, in order to quickly adapt to the complex environment. For example, when there are unruly human drivers (regarded as physical attackers) disrupting an autonomous vehicle platoon, safety distance between autonomous vehicles should adapt to mitigate such attacks. Here the safety distance is influenced by the presence of physical attackers, which is not simply constant or time-varying, but instead are *environment-aware and dynamic*.

B. Related Work

There are studies considering cooperative target tracking control for multi-agent systems. For example, [21] proposes a cooperative target fencing control framework for multiple unmanned aerial vehicles. However, this work does not account for constraint requirements on the vehicles. In [22], authors employ a distance-based formation control with a collision-avoidance potential function to tackle the collaborative target tracking problem for multiple autonomous surface vehicles. However, this method cannot deal with the cooperative target tracking problem when the number of agents exceeds three. The work in [23] presents a target fencing control strategy for multiple vehicles, but it only addresses constant constraint requirements. In [24], BLFs are used to address safety constraint requirements for each agent with its neighboring agents rather than all other agents. This limitation implies that collision avoidance and connectivity between an agent and rest of the group may not be guaranteed during the target tracking operation. A safety-critical cooperative target enclosing control framework for multiple unmanned surface vehicles is proposed in [25] to handle multiple constant constraint requirements which requires high computation cost and faces feasibility problem. In conclusion, none of these studies can handle the cooperative target tracking problem of multi-agent systems with *environment-aware and dynamic* constraint requirements, especially in the presence of physical attackers.

C. Contributions

This article considers a 3D cooperative target tracking problem by a team of autonomous agents with multiple constraint requirements, in the face of multiple physical attackers. The goal is to enable agents to perform centriod-based target tracking (i.e., cooperative target tracking) while maintaining desired inter-agent distances (i.e., formation tracking). Under the proposed control framework, formation tracking errors for the agents are uniformly ultimately bounded, with all constraint requirements met.

The main contributions can be summarized as follows:

- **Environment-aware and dynamic constraints:** In this work, the performance constraint requires that the centriod of agents needs to be close to the target. However, when attackers move close to the target, agents must prioritize safety by retreating from the target to avoid collisions with attackers. In such a scenario, a constant or time-varying performance constraint may conflict with the safety constraint requirements. To address this issue, the proposed control framework introduces an *environment-aware and dynamic* performance constraint function that can be relaxed when the target is close to attackers. See Remarks 5 and 7, and control objective (CO4) for more discussion. Moreover, in this work safety constraint requirements on inter-agent distances depend on the distances from attackers, hence *environment-aware and dynamic*. This consideration is inspired by the concept of "cohesion tactics" [26], a behavior observed in certain species, such as antelopes and zebras. In such species, individuals instinctively stay close together to enhance safety and protection, thereby decreasing the risk of being hunted by predators. Similarly, our approach adopts this principle to enhance group cohesion and improve resilience in the presence of attackers. See Remark 6, and control objective (CO3) for more discussion.
- **Intelligent behavior modeling:** In this work, the target and attackers possess intelligence and can adjust velocities based on relative coordinates with the agents and agents' velocities. Thus, [23], [24], [25], [27], which consider target and obstacles with time-varying velocity are inadequate in addressing the cooperative target tracking problem considered in this work. See Assumptions 3 and 4, and Remarks 2 and 3 for more discussion.
- **Neural network-based adaptive constrained control framework:** Universal barrier function (UBF) is utilized to address different constraint requirements in a unified framework. Adaptive laws integrated with radical basis function neural networks (RBFNNs) are designed to estimate the unknown attacker and target velocities.

D. Difference

Recently there has been some work on "adaptive safety" using control barrier functions [28], [29], [30], [31], where the word "adaptive" means "adaptation" to parametric system uncertainties. These approaches use constant or time-varying safe sets, which differ fundamentally from the *environment-aware and dynamic constraints* that respond to physical attackers.

It is also worth noting that the cooperative target tracking problem in this work differs from traditional multi-player/multi-agent pursuit-evasion games [32], [33], [34]:

- Pursuit-evasion games aim to obtain optimal strategic policies for all players. Whereas in this work, the target and attackers cannot be controlled, and the control design is focused on the agents.
- Existing pursuit-evasion strategies cannot effectively deal with *environment-aware and dynamic* constraint requirements in the presence of intelligent physical attackers.

The problem here is also different from multi-agent planning in dynamic environment [35], [36], [37] and multi-agent formation with dynamic obstacles [38], [39], [40], [41]. Major differences include:

- Planning alone cannot guarantee that the multi-agent system can perfectly track the planned trajectory/formation at all time. In this work, consideration of dynamic environment due to physical attackers is integrated into the *environment-aware and dynamic* constraint requirements, so as to ensure satisfaction of constraints at all time.
- "Dynamic environment/obstacles" in the aforementioned literature only addresses static or time-varying environment obstacles, where the environment is independent of the multi-agent system. In this work, the physical attackers are dynamic and adjust their velocities based on relative coordinates with agents and agents' velocities.

E. Organization

The remainder of this work is organized as follows. Section II presents notations and lemmas. Section III gives problem formulation including system kinematics, introduction of agent and attacker sets, and control objective. Section IV introduces radical basis function neural networks and universal barrier function, followed by the controller design and theoretic analysis. Section V presents simulation studies to illustrate the theoretical results. The Appendix contains some algebraic details and proof procedures for the related proposition.

II. Notations and Lemmas

A. Notations

Let $\mathbb{R}$ and $\mathbb{R}^+$ be the real and positive number sets, respectively. Define $\mathbb{R}_{\geq 0} \triangleq \mathbb{R}^+ \cup \{0\}$, and let I_m denote the $m \times m$ identity matrix. Moreover, $(\cdot)^{\mathrm{T}}$ is the transpose of $(\cdot)$, $|\cdot|$ represents absolute values for scalars, and $\|\cdot\|$ represents Euclidean norms for vectors and induced norms for matrices. In addition, $\otimes$ represents the Kronecker product. For any matrix $A \in \mathbb{R}^{n\times m}$ where $A = [A_1, \cdots, A_m]$ and $A_j \in \mathbb{R}^n$, $j = 1, \cdots, m$, the vector operator $\mathrm{vec}(\cdot)$ gives $\mathrm{vec}(A) = [A_1^{\mathrm{T}}, \cdots, A_m^{\mathrm{T}}]^{\mathrm{T}} \in \mathbb{R}^{nm}$. Furthermore, $\mathbb{S}^2 = \{x \in \mathbb{R}^3 \mid \|x\| = 1\}$ is a set of unit vectors in $\mathbb{R}^3$. The distance between $q_1 \in \mathbb{R}^3$ and $q_2 \in \mathbb{R}^3$ is defined as $\mathrm{dist}(q_1, q_2) \triangleq \|q_1 - q_2\|$, the distance between a point $q_1 \in \mathbb{R}^3$ and a set $\mathcal{S}_1 \subseteq \mathbb{R}^3$ is defined as $\mathrm{dist}(q_1, \mathcal{S}_1) \triangleq \inf\{\|q_1 - \zeta_1\| \big| \zeta_1 \in \mathcal{S}_1\}$, and the distance between two sets $\mathcal{S}_1 \subseteq \mathbb{R}^3$ and $\mathcal{S}_2 \subseteq \mathbb{R}^3$ is defined as $\mathrm{dist}(\mathcal{S}_1, \mathcal{S}_2) \triangleq \inf\{\|\zeta_1 - \zeta_2\| \big| \zeta_1 \in \mathcal{S}_1, \zeta_2 \in \mathcal{S}_2\}$.

B. Lemmas

The following lemmas are required.

Lemma 1: ([42]) Let $A \in \mathbb{R}^{n\times m}$, $B \in \mathbb{R}^{m\times l}$, and $C \in \mathbb{R}^{l\times k}$. Then $\mathrm{vec}(ABC) = (C^{\mathrm{T}} \otimes A)\mathrm{vec}(B)$.

For the next lemma, let $\rho > 0$, and consider $\mathrm{softmin}_\rho : \mathbb{R} \times \cdots \times \mathbb{R} \to \mathbb{R}$ and $\mathrm{softmax}_\rho : \mathbb{R} \times \cdots \times \mathbb{R} \to \mathbb{R}$ defined by

$$\mathrm{softmin}_\rho(d_1, \cdots, d_N) \triangleq -\frac{1}{\rho}\ln\left[\sum_{i=1}^{N}\exp(-\rho d_i)\right],$$

$$\mathrm{softmax}_\rho(d_1, \cdots, d_N) \triangleq \frac{1}{\rho}\ln\left[\sum_{i=1}^{N}\exp(\rho d_i)\right],$$

which are continuously differentiable with respect to d_i ($i = 1, \cdots, N$).

Lemma 2: ([43], [44], [45]) Let $d_1, \ldots, d_N \in \mathbb{R}$. Then, the following statements hold:

1) $\mathrm{softmin}_\rho(d_1, \cdots, d_N) \leq \min\{d_1, \cdots, d_N\}$.
2) $\max\{d_1, \cdots, d_N\} \leq \mathrm{softmax}_\rho(d_1, \cdots, d_N)$.
3) $\lim_{\rho\to\infty} \mathrm{softmin}_\rho(d_1, \cdots, d_N) = \min\{d_1, \cdots, d_N\}$.
4) $\lim_{\rho\to\infty} \mathrm{softmax}_\rho(d_1, \cdots, d_N) = \max\{d_1, \cdots, d_N\}$.

In other words, $\mathrm{softmin}_\rho$ and $\mathrm{softmax}_\rho$ are smooth approximations of the minimum and maximum, respectively.

III. Problem Formulation

A. System Kinematics

In this subsection, we introduce kinematics for agents, the target, and physical attackers.

First, consider $N_{\mathrm{u}} \geq 2$ agents in the multi-agent system (for example, unmanned aerial vehicles), where any two agents can communicate with each other. The ith agent ($i = 1, \cdots, N_{\mathrm{u}}$) has the following kinematics

$$\dot{q}_i(t) = p_i(t) + \xi_i(t), \quad q_i(0) = q_{i0}, \tag{1}$$

where $t \geq 0$, $q_{i0} \in \mathbb{R}^3$ is the initial position, $q_i(t) \in \mathbb{R}^3$ and $p_i(t) \in \mathbb{R}^3$ are the agent's position and control, respectively. Moreover, $\xi_i(t) \in \mathbb{R}^3$ is the external disturbance. Unless otherwise stated, the subscripts i and j used in this work belongs to the set $i, j \in \{1, \cdots, N_{\mathrm{u}}\}$, $j \neq i$.

Assumption 1: ([46], [47]) The external disturbance ξ_i is continuous with *unknown* bound (i.e., there exists a positive constant $\bar{\xi}_i$ such that $\|\xi_i\| \leq \bar{\xi}_i$).

Assumption 2: ([48], [49], [50], [51]) $\|p_i\| > 0$.

Remark 1: Assumption 2 comes from practical considerations and is commonly adopted in literature addressing autonomous vehicles [48], [51], surface/underwater ships [49], and fixed-wing aerial vehicles [50], etc.

The target to be tracked by agents has the kinematics

$$\dot{q}_{\mathrm{t}}(t) = p_{\mathrm{t}}(t), \quad q_{\mathrm{t}}(0) = q_{\mathrm{t}0}, \tag{2}$$

where $t \geq 0$, $q_{\mathrm{t}0} \in \mathbb{R}^3$ is the initial position, $q_{\mathrm{t}}(t) \in \mathbb{R}^3$ and $p_{\mathrm{t}}(t) \in \mathbb{R}^3$ are the target's position and velocity, respectively.

Assumption 3: The target's velocity p_{t} is continuous, subject to saturation, and dependents on agents' velocities and relative positions. Specifically,

$$p_{\mathrm{t}} = \mathrm{sat}(u_{\mathrm{t}}(Z_{\mathrm{t}})) = \begin{cases} \bar{p}_{\mathrm{t}}\dfrac{u_{\mathrm{t}}(Z_{\mathrm{t}})}{\|u_{\mathrm{t}}(Z_{\mathrm{t}})\|}, & \|u_{\mathrm{t}}(Z_{\mathrm{t}})\| \geq \bar{p}_{\mathrm{t}}, \\ u_{\mathrm{t}}(Z_{\mathrm{t}}), & \|u_{\mathrm{t}}(Z_{\mathrm{t}})\| < \bar{p}_{\mathrm{t}}, \end{cases}$$

where $Z_{\mathrm{t}} = [\cdots, \underbrace{\dot{q}_i^{\mathrm{T}}, (q_i - q_{\mathrm{t}})^{\mathrm{T}}}_{i=1,\cdots,N_{\mathrm{u}}}, \cdots]^{\mathrm{T}} \in \mathbb{R}^{6N_{\mathrm{u}}}$, $u_{\mathrm{t}} : \mathbb{R}^{6N_{\mathrm{u}}} \to \mathbb{R}^3$, and $\bar{p}_{\mathrm{t}} > 0$ is the target's maximum speed. Furthermore, p_{t} and $\bar{p}_{\mathrm{t}}$ are *unknown*.

Remark 2: Assumption 3 indicates that the target is intelligent. Define the centriod of all agents as $q_{\mathrm{c}} \triangleq \frac{1}{N_{\mathrm{u}}}\sum_{i=1}^{N_{\mathrm{u}}} q_i$. For instance, if the target wants to escape from q_{c}, then it can select its strategy as $u_{\mathrm{t}} = \dot{q}_{\mathrm{c}} - K_{\mathrm{t}}(q_{\mathrm{c}} - q_{\mathrm{t}})$ and $p_{\mathrm{t}} = \mathrm{sat}(u_{\mathrm{t}})$,

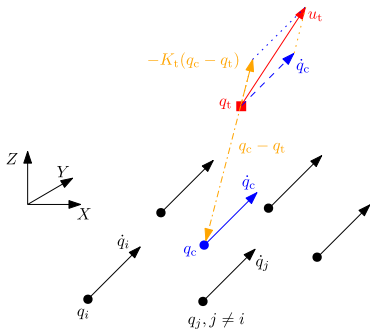

Fig. 1. A graphical illustration for the target velocity in Remark 2.

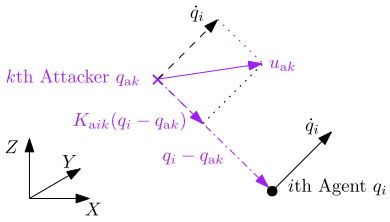

Fig. 2. A graphical illustration for the kth attacker velocity in Remark 3.

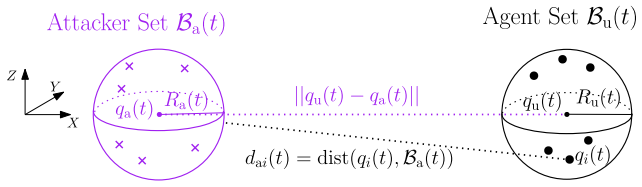

Fig. 3. A graphical illustration for agent set $\mathcal{B}_u(t)$ and attacker set $\mathcal{B}_a(t)$ where purple crosses represent positions of attackers and black dots represent positions of agents.

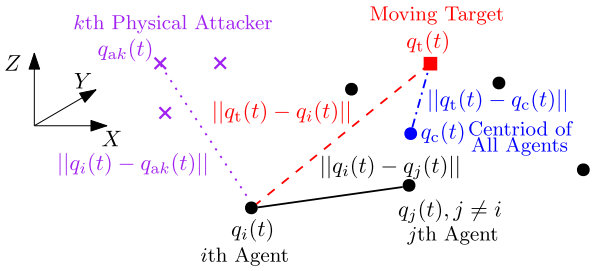

Fig. 4. A brief graphical illustration for multi-agents' cooperative target tracking in the presence of multiple physical attackers.

where $K_t > 0$, as illustrated in Figure 1. Control frameworks considering the moving targets with either unknown constant velocity [23] or time-varying velocity [24], [25], [27] are inadequate in addressing the cooperative target tracking problem in this work.

To disrupt the multi-agent system target tracking operation, $N_a \geq 2$ physical attackers are present, where the kth attacker ($k = 1, \cdots, N_a$) has the kinematics

$$\dot{q}_{ak}(t) = p_{ak}(t), \quad q_{ak}(0) = q_{ak0}, \tag{3}$$

where $t \geq 0$, $q_{ak0} \in \mathbb{R}^3$ is the initial position, $q_{ak}(t) \in \mathbb{R}^3$ and $p_{ak}(t) \in \mathbb{R}^3$ are the position and velocity, respectively. Unless otherwise stated, subscript k used in this work belongs to the set $k \in \{1, \cdots, N_a\}$.

Assumption 4: The kth attacker's velocity p_{ak} is continuous, subject to saturation, and depends on agents' velocities and relative positions. Specifically,

$$\begin{aligned} p_{ak} &= \text{sat}(u_{ak}(Z_{ak})) \\ &= \begin{cases} \bar{p}_{ak} \dfrac{u_{ak}(Z_{ak})}{\|u_{ak}(Z_{ak})\|}, & \|u_{ak}(Z_{ak})\| \geq \bar{p}_{ak}, \\ u_{ak}(Z_{ak}), & \|u_{ak}(Z_{ak})\| < \bar{p}_{ak}, \end{cases} \end{aligned}$$

where $Z_{ak} = [\underbrace{\cdots, \dot{q}_i^{\mathrm{T}}, (q_i - q_{ak})^{\mathrm{T}}, \cdots}_{i=1,\cdots,N_u}]^{\mathrm{T}} \in \mathbb{R}^{6N_u}$, $u_{ak} : \mathbb{R}^{6N_u} \to \mathbb{R}^3$, and $\bar{p}_{ak} > 0$ is the kth attacker's maximum speed. Furthermore, p_{ak} and $\bar{p}_{ak}$ are *unknown*.

Remark 3: Assumption 4 means the attackers are intelligent. For instance, if the kth attacker intends to collide with the ith agent, then it can choose its attack strategy as $u_{ak} = \dot{q}_i + K_{ak}(q_i - q_{ak})$ and $p_{ak} = \text{sat}(u_{ak})$, where $K_{ak} > 0$, which is a strategy similar to the hawk's hunting/catching behavior in nature [52] (Figure 2). Well-established obstacle-avoidance mechanisms that only consider static or time-varying obstacles [38], [39], [40], [41] cannot effectively deal with such intelligent attackers.

Assumption 5: Agents can detect positions of the target and attackers.

Remark 4: This assumption is commonly used in work that considers collision avoidance such as [53], [54], and [55]. In practice, this assumption can be met by implementing devices such as cameras and LiDAR sensors on the agents.

B. Agent and Attacker Sets

In practice, agents and attackers exhibit swarm behaviors. Therefore, we introduce sets (balls) for agents and attackers. Specifically, for all $t \geq 0$, define $\mathcal{B}_u(t) \subseteq \mathbb{R}^3$ and $\mathcal{B}_a(t) \subseteq \mathbb{R}^3$ to include N_u agents and N_a attackers, respectively. See Figure 3 for an illustration (the target is omitted in Figure 3 for graphical simplicity), where expressions for the set centers $q_u(t)$ and $q_a(t)$ are given in (35) and (37) in Appendix A, and expressions for the radii $R_u(t)$ and $R_a(t)$ are given in (36) and (38) in Appendix A.

C. Control Objective

To track the target cooperatively, the agents need to fence the target with a desired formation in the presence of physical attackers (Figure 4), subject to multiple safety and performance constraints. Specifically, let $\Omega_a \in \mathbb{R}^+$ and $\Omega_{ti} \in \mathbb{R}^+$, such that $\Omega_a < \|q_u(0) - q_a(0)\| - R_u(0) - R_a(0)$ and $\Omega_{ti} < \|q_t(0) - q_i(0)\|$. Moreover, define $d_{ai} \triangleq \text{dist}(q_i, \mathcal{B}_a)$, and let $d_{dij}(d_{ai}, d_{aj}) : \mathbb{R}_{\geq 0} \times \mathbb{R}_{\geq 0} \to \mathbb{R}^+$ be the desired distance between the ith and jth agents, which is at least once continuously differentiable with bounded partial derivatives. Let $\Omega_{Hij}(d_{ai}, d_{aj}) : \mathbb{R}_{\geq 0} \times \mathbb{R}_{\geq 0} \to \mathbb{R}^+$ and $\Omega_{Lij}(d_{ai}, d_{aj}) : \mathbb{R}_{\geq 0} \times \mathbb{R}_{\geq 0} \to \mathbb{R}^+$, which are at least once continuously differentiable with bounded partial derivatives, such that $\Omega_{Lij} < d_{dij} < \Omega_{Hij}$ and $\Omega_{Lij}(d_{ai}(0), d_{aj}(0)) < \|q_i(0) - q_j(0)\| < \Omega_{Hij}(d_{ai}(0), d_{aj}(0))$. Furthermore, let $\omega_{tc}(t) : \mathbb{R}_{\geq 0} \to \mathbb{R}^+$ be bounded and

at least once continuously differentiable with bounded time derivatives, such that $\|q_{\rm c}(0) - q_{\rm t}(0)\| < \omega_{\rm tc}(0)$. Finally, let $\Omega_{d{\rm tc}}(\omega_{\rm tc}, R_{\rm a}, \Omega_{\rm a}, q_{\rm t}, q_{\rm a}) : \mathbb{R}^+ \times \mathbb{R}^+ \times \mathbb{R}^+ \times \mathbb{R}^3 \times \mathbb{R}^3 \to \mathbb{R}^+$ be at least once continuously differentiable with bounded partial derivatives, such that $\Omega_{d{\rm tc}} > R_{\rm a} + \Omega_{\rm a} - \|q_{\rm t} - q_{\rm a}\|$ and $\|q_{\rm c}(0) - q_{\rm t}(0)\| < \Omega_{d{\rm tc}}(\omega_{\rm tc}(0), R_{\rm a}(0), \Omega_{\rm a}, q_{\rm t}(0), q_{\rm a}(0))$.

The **control objective** is to design a control framework for the agents such that

(CO1) $\|q_{\rm u} - q_{\rm a}\| > R_{\rm u} + R_{\rm a} + \Omega_{\rm a}$, $\forall t \geq 0$;
(CO2) $\|q_i - q_{\rm t}\| > \Omega_{{\rm t}i}$, $\forall t \geq 0$;
(CO3) $\Omega_{{\rm L}ij}(d_{{\rm a}i}, d_{{\rm a}j}) < \|q_i - q_j\| < \Omega_{{\rm H}ij}(d_{{\rm a}i}, d_{{\rm a}j})$, $\forall t \geq 0$;
(CO4) $\|q_{\rm c} - q_{\rm t}\| < \Omega_{d{\rm tc}}(\omega_{\rm tc}, R_{\rm a}, \Omega_{\rm a}, q_{\rm t}, q_{\rm a})$, $\forall t \geq 0$.
(CO5) There exists $\epsilon > 0$ such that $\limsup_{t\to\infty} \left|\|q_i - q_j\| - d_{{\rm d}ij}(d_{{\rm a}i}, d_{{\rm a}j})\right| \leq \epsilon$, and ϵ can be made arbitrarily small by choice of control parameters.

Control objectives (CO1)–(CO3) are different *safety constraint* requirements. Specifically, (CO1) requires that agents keep a safe distance from attackers. (CO2) requires that the ith agent avoids collision with the target. (CO3) requires that inter-agent distances cannot be either too small or too large. In addition, (CO4) is a *performance* requirement, which requires the centroid of the agents should not be far away from the target. Finally, (CO5) requires that the formation tracking error between the ith and jth agents can converge into a region close to zero as time approaches infinity.

Proposition 1: If (CO1) is satisfied, then $\|q_{\rm c} - q_{\rm t}\| > R_{\rm a} + \Omega_{\rm a} - \|q_{\rm t} - q_{\rm a}\|$.

Proof: See Appendix B. ∎

Remark 5: Proposition 1 implies that if the target is near to or enclosed by attackers, then the centroid of all agents cannot be arbitrarily close to the target because of (CO1). This means (CO1) (safety) has a higher priority over (CO4) (performance). See Remark 7 for further discussion.

Remark 6: It is worth noting that (CO3) involves *environment-aware and dynamic* safety constraint requirements, which are attacker-dependent and can adapt to the complex operation environment. Same is true for the desired inter-agent distance $d_{{\rm d}ij}(d_{{\rm a}i}, d_{{\rm a}j})$. For instance, when attackers are nearby, agents can employ a more compact formation to avoid the attackers. Therefore, as attackers get closer, the desired inter-agent distances need to decrease, and the region $(\Omega_{{\rm L}ij},\ \Omega_{{\rm H}ij})$ in (CO3) needs to become smaller. In this case, let $l_{{\rm d}ij} \in \mathbb{R}^+$, $\lambda_{ij} \in (0, 1)$, $\alpha_{ij} \in \mathbb{R}^+$, $\iota \in \mathbb{R}^+$, $\bar{\Omega}_{ij} \in \mathbb{R}^+$, and $\underline{\Omega}_{ij} \in \mathbb{R}^+$, such that $0 < \underline{\Omega}_{ij} < \underline{\Omega}_{ij} + 2\iota < \bar{\Omega}_{ij}$. We can select $d_{{\rm d}ij}$ as

$$d_{{\rm d}ij} = l_{{\rm d}ij} + \frac{l_{{\rm d}ij}(\lambda_{ij} - 1)}{2}\left[\exp(-\alpha_{ij} d_{{\rm a}i}) + \exp(-\alpha_{ij} d_{{\rm a}j})\right],$$

such that

$$\lim_{d_{{\rm a}i}, d_{{\rm a}j} \to \infty} d_{{\rm d}ij} = l_{{\rm d}ij}, \qquad \lim_{d_{{\rm a}i}, d_{{\rm a}j} \to 0} d_{{\rm d}ij} = \lambda_{ij} l_{{\rm d}ij} < l_{{\rm d}ij}.$$

In (CO3) we can select

$$\Omega_{{\rm H}ij} = \bar{\Omega}_{ij} - \frac{\iota}{2}\left[\exp(-\alpha_{ij} d_{{\rm a}i}) + \exp(-\alpha_{ij} d_{{\rm a}j})\right],$$
$$\Omega_{{\rm L}ij} = \underline{\Omega}_{ij} + \frac{\iota}{2}\left[\exp(-\alpha_{ij} d_{{\rm a}i}) + \exp(-\alpha_{ij} d_{{\rm a}j})\right],$$

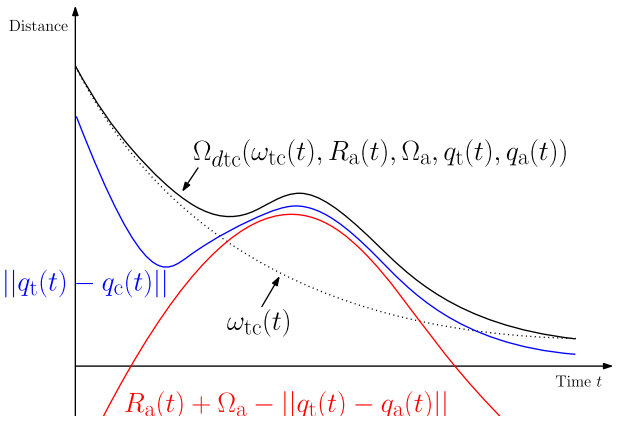

Fig. 5. A graphical illustration for the performance constraint function in Remark 7. When $R_{\rm a} + \Omega_{\rm a} - \|q_{\rm t} - q_{\rm a}\| < \omega_{\rm tc}$, the performance constraint function $\Omega_{d{\rm tc}}(\omega_{\rm tc}, R_{\rm a}, \Omega_{\rm a}, q_{\rm t}, q_{\rm a})$ is close to the user-defined time-varying function $\omega_{\rm tc}$.

such that

$$\lim_{d_{{\rm a}i}, d_{{\rm a}j} \to \infty} \Omega_{{\rm H}ij} = \bar{\Omega}_{ij}, \quad \lim_{d_{{\rm a}i}, d_{{\rm a}j} \to \infty} \Omega_{{\rm L}ij} = \underline{\Omega}_{ij},$$
$$\lim_{d_{{\rm a}i}, d_{{\rm a}j} \to 0} \Omega_{{\rm H}ij} = \bar{\Omega}_{ij} - \iota, \quad \lim_{d_{{\rm a}i}, d_{{\rm a}j} \to 0} \Omega_{{\rm L}ij} = \underline{\Omega}_{ij} + \iota.$$

Remark 7: (CO4) involves an *environment-aware and dynamic* performance constraint requirement. Note that due to Proposition 1, if we only require $\|q_{\rm c} - q_{\rm t}\| < \omega_{\rm tc}$ for some time-varying $\omega_{\rm tc}$, a conflict between (CO1) and (CO4) can occur when $\omega_{\rm tc} < R_{\rm a} + \Omega_{\rm a} - \|q_{\rm t} - q_{\rm a}\|$. Hence, the design of performance constraint in (CO4) needs to take attacker positions into consideration, i.e., if attackers are close to the target, agents need to move away from the target in order to avoid collisions with attackers. In this case, let $\mu_{\rm tc} \in \mathbb{R}^+$ and $\rho_{\rm tc} \in \mathbb{R}^+$, we can design $\Omega_{d{\rm tc}}$ as $\Omega_{d{\rm tc}}(\omega_{\rm tc}, R_{\rm a}, \Omega_{\rm a}, q_{\rm t}, q_{\rm a}) = \text{softmax}_{\rho_{\rm tc}}\big(R_{\rm a} + \Omega_{\rm a} - \tanh(\|q_{\rm t} - q_{\rm a}\|)\|q_{\rm t} - q_{\rm a}\| + \mu_{\rm tc},\ \omega_{\rm tc}\big)$. A graphical illustration of this design is shown in Figure 5.

Remark 8: The control objective (CO5) implies that the formation operation in this work aims to maintain desired inter-agent distances but does not prescribe a fixed geometric pattern in a global coordinate frame. Thus, the term "formation" in this work refers specifically to a "distance-based formation" [22], [56], [57], [58]. When (CO5) is satisfied, the overall formation may undergo translation or rotation while preserving its internal structure.

IV. Controller Design and Main Results

A. Radical Basis Function Neural Networks (RBFNNs)

We will use RBFNNs [59], [60], [61], [62], [63] to estimate unknown velocities of the target and each attacker. Specifically, for continuous nonlinear functions $p_{\rm t}$ and p_{ak} defined over a compact set $S_{Z{\rm t}} \subset \mathbb{R}^{6N_{\rm u}}$ and $S_{Zak} \subset \mathbb{R}^{6N_{\rm u}}$, respectively, there exist corresponding RBFNNs $W_{\rm t}^{\rm T} B_{\rm t}$ and $W_{ak}^{\rm T} B_{ak}$ given as

$$\begin{aligned} p_{\rm t} &= W_{\rm t}^{\rm T} B_{\rm t}(Z_{\rm t}) + \epsilon_{\rm t}(Z_{\rm t}), \\ p_{ak} &= W_{ak}^{\rm T} B_{ak}(Z_{ak}) + \epsilon_{ak}(Z_{ak}), \end{aligned} \tag{4}$$

where $W_{\rm t} \in \mathbb{R}^{\gamma \times 3}$ and $W_{ak} \in \mathbb{R}^{\gamma \times 3}$ are ideal weight matrices, with $\gamma \geq 1$ being the number of neural network nodes, $B_{\rm t}(Z_{\rm t}) = [b_1(Z_{\rm t}), \cdots, b_\gamma(Z_{\rm t})]^{\rm T} \in \mathbb{R}^\gamma$ and $B_{ak}(Z_{ak}) =$

$[b_{k1}(Z_{ak}), \cdots, b_{k\gamma}(Z_{ak})]^{\mathrm{T}} \in \mathbb{R}^{\gamma}$ are basis function vectors, and $\epsilon_{\mathrm{t}}(Z_{\mathrm{t}}) \in \mathbb{R}^3$ and $\epsilon_{ak}(Z_{ak}) \in \mathbb{R}^3$ are approximation errors satisfying $\|\epsilon_{\mathrm{t}}\| \leq \bar{\epsilon}_{\mathrm{t}}$ and $\|\epsilon_{ak}\| \leq \bar{\epsilon}_{ak}$, where $\bar{\epsilon}_{\mathrm{t}} > 0$ and $\bar{\epsilon}_{ak} > 0$ are given precision levels. The basis functions $b_l(Z_{\mathrm{t}})$ and $b_{kl}(Z_{ak})$ are selected as the following Gaussian-like functions [64], [65]

$$b_l(Z_{\mathrm{t}}) = \exp\left[-\frac{(Z_{\mathrm{t}} - \nu_l)^{\mathrm{T}}(Z_{\mathrm{t}} - \nu_l)}{\zeta_l^2}\right],$$
$$b_{kl}(Z_{ak}) = \exp\left[-\frac{(Z_{ak} - \nu_{kl})^{\mathrm{T}}(Z_{ak} - \nu_{kl})}{\zeta_{kl}^2}\right],$$

with $\nu_l \in \mathbb{R}^{6N_{\mathrm{u}}}$ and $\nu_{kl} \in \mathbb{R}^{6N_{\mathrm{u}}}$ being the receptive field's center and $\zeta_l \in \mathbb{R}$ and $\zeta_{kl} \in \mathbb{R}$ being the width of the Gaussian-like functions $b_l(Z_{\mathrm{t}})$ and $b_{kl}(Z_{ak})$, respectively.

B. Universal Barrier Function

First, define $d_{\mathrm{au}} \triangleq \|q_{\mathrm{u}} - q_{\mathrm{a}}\|$, $\Omega_{\mathrm{au}} \triangleq R_{\mathrm{u}} + R_{\mathrm{a}} + \Omega_{\mathrm{a}}$, and $d_{ti} \triangleq \|q_{\mathrm{t}} - q_i\|$. To address the safety constraints in (CO1) and (CO2), the following transformed variables are introduced:

$$\eta_{\mathrm{au}} = \frac{1}{d_{\mathrm{au}} - \Omega_{\mathrm{au}}}, \quad \eta_{ti} = \frac{1}{d_{ti} - \Omega_{ti}}. \tag{5}$$

Moreover, define $d_{eij} \triangleq \|q_i - q_j\| - d_{\mathrm{d}ij}$, $\Omega_{\mathrm{eL}ij} \triangleq d_{\mathrm{d}ij} - \Omega_{\mathrm{L}ij}$, and $\Omega_{\mathrm{eH}ij} \triangleq \Omega_{\mathrm{H}ij} - d_{\mathrm{d}ij}$. Control objective (CO3) is equivalent to

$$-\Omega_{\mathrm{eL}ij} < d_{eij} < \Omega_{\mathrm{eH}ij}. \tag{6}$$

Hence, a transformed variable is designed as

$$\eta_{eij} = \frac{\Omega_{\mathrm{eH}ij}\Omega_{\mathrm{eL}ij}d_{eij}}{(\Omega_{\mathrm{eH}ij} - d_{eij})(\Omega_{\mathrm{eL}ij} + d_{eij})}. \tag{7}$$

Next, we will consider a transformed variable for the performance constraint requirement in (CO4). As well documented in the literature [66], [67], [68], using target fencing error $\|q_{\mathrm{t}} - q_{\mathrm{c}}\|$ directly in the controller design will cause singularity issues, since its derivative yields $\frac{\mathrm{d}(\|q_{\mathrm{t}} - q_{\mathrm{c}}\|)}{\mathrm{d}t} = \frac{1}{\|q_{\mathrm{t}} - q_{\mathrm{c}}\|}(q_{\mathrm{c}} - q_{\mathrm{t}})^{\mathrm{T}}(\dot{q}_{\mathrm{c}} - \dot{q}_{\mathrm{t}})$, which is not continuous when $\|q_{\mathrm{t}} - q_{\mathrm{c}}\| = 0$. To bypass such a problem, define $D_{\mathrm{tc}} \triangleq \frac{1}{2}\|q_{\mathrm{t}} - q_{\mathrm{c}}\|^2$ and $\Omega_{D\mathrm{tc}} \triangleq \frac{1}{2}\Omega_{d\mathrm{tc}}^2$. The performance constraint requirement in (CO4) is equivalent to

$$D_{\mathrm{tc}} < \Omega_{D\mathrm{tc}}. \tag{8}$$

Therefore, we can design the following transformed variable

$$\Pi_{\mathrm{tc}} = \frac{\Omega_{D\mathrm{tc}} D_{\mathrm{tc}}}{\Omega_{D\mathrm{tc}} - D_{\mathrm{tc}}}. \tag{9}$$

Now, we design the UBF as

$$V_q = \Pi_{\mathrm{tc}} + \frac{1}{2}\eta_{\mathrm{au}}^2 + \sum_{i=1}^{N_{\mathrm{u}}}\left(\frac{1}{2}\eta_{ti}^2 + \sum_{j=1, j\neq i}^{N_{\mathrm{u}}}\frac{1}{2}\eta_{eij}^2\right). \tag{10}$$

If V_q in (10) is shown to be uniformly bounded through closed-loop analysis, it implies that the transformed variables Π_{tc}, η_{au}, η_{ti}, and η_{eij} are uniformly bounded, which then implies that the control objectives (CO1)-(CO4) are satisfied.

More discussion on the UBF and how it compares with other barrier structures can be seen in details in [69].

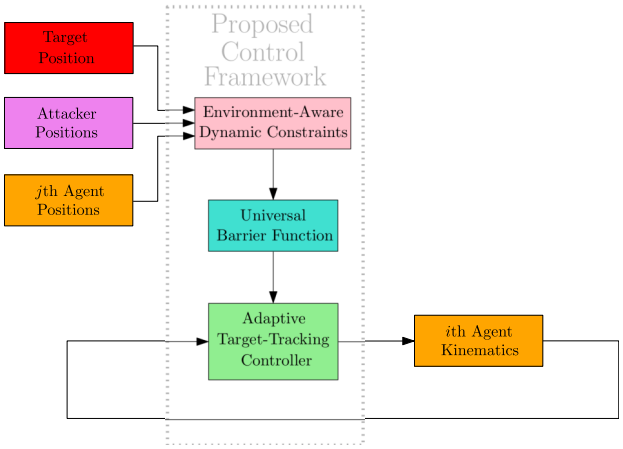

Fig. 6. High-level block diagram of the overall control framework.

C. Analysis and Main Results

Here we present the cooperative target tracking controller design and main theoretical results. Figure 6 presents a brief overview of the proposed control framework.

For $\dot{V}_q$, from (10) we have

$$\dot{V}_q = \dot{\Pi}_{\mathrm{tc}} + \eta_{\mathrm{au}}\dot{\eta}_{\mathrm{au}} + \sum_{i=1}^{N_{\mathrm{u}}}\left(\eta_{ti}\dot{\eta}_{ti} + \sum_{j=1, j\neq i}^{N_{\mathrm{u}}}\eta_{eij}\dot{\eta}_{eij}\right). \tag{11}$$

We will analyze the terms in (11) sequentially. First, in (11), $\dot{\Pi}_{\mathrm{tc}}$ can be written as

$$\dot{\Pi}_{\mathrm{tc}} = \left(\sum_{i=1}^{N_{\mathrm{u}}}\frac{\partial \Pi_{\mathrm{tc}}}{\partial q_i}\dot{q}_i\right) + \frac{\partial \Pi_{\mathrm{tc}}}{\partial q_{\mathrm{t}}}\dot{q}_{\mathrm{t}} + \frac{\partial \Pi_{\mathrm{tc}}}{\partial \omega_{\mathrm{tc}}}\dot{\omega}_{\mathrm{tc}} + \left(\sum_{k=1}^{N_{\mathrm{a}}}\frac{\partial \Pi_{\mathrm{tc}}}{\partial q_{ak}}\dot{q}_{ak}\right), \tag{12}$$

where

$$\frac{\partial \Pi_{\mathrm{tc}}}{\partial q_i} = -\frac{1}{N_{\mathrm{u}}}\frac{\partial \Pi_{\mathrm{tc}}}{\partial D_{\mathrm{tc}}}(q_{\mathrm{t}} - q_{\mathrm{c}})^{\mathrm{T}},$$
$$\frac{\partial \Pi_{\mathrm{tc}}}{\partial q_{\mathrm{t}}} = \frac{\partial \Pi_{\mathrm{tc}}}{\partial D_{\mathrm{tc}}}(q_{\mathrm{t}} - q_{\mathrm{c}})^{\mathrm{T}} + \frac{\partial \Pi_{\mathrm{tc}}}{\partial \Omega_{D\mathrm{tc}}}\Omega_{d\mathrm{tc}}\frac{\partial \Omega_{d\mathrm{tc}}}{\partial q_{\mathrm{t}}},$$
$$\frac{\partial \Pi_{\mathrm{tc}}}{\partial \omega_{\mathrm{tc}}} = \frac{\partial \Pi_{\mathrm{tc}}}{\partial \Omega_{D\mathrm{tc}}}\Omega_{d\mathrm{tc}}\frac{\partial \Omega_{d\mathrm{tc}}}{\partial \omega_{\mathrm{tc}}},$$
$$\frac{\partial \Pi_{\mathrm{tc}}}{\partial q_{ak}} = \Omega_{d\mathrm{tc}}\frac{\partial \Pi_{\mathrm{tc}}}{\partial \Omega_{D\mathrm{tc}}}\left(\frac{\partial \Omega_{d\mathrm{tc}}}{\partial R_{\mathrm{a}}}\frac{\partial R_{\mathrm{a}}}{\partial q_{ak}} + \frac{\partial \Omega_{d\mathrm{tc}}}{\partial q_{\mathrm{a}}}\frac{\partial q_{\mathrm{a}}}{\partial q_{ak}}\right).$$

Furthermore, let $E_{\mathrm{au}} \triangleq \frac{q_{\mathrm{u}} - q_{\mathrm{a}}}{d_{\mathrm{au}}} \in \mathbb{S}^2$, taking time derivative of η_{au} in (11) yields

$$\dot{\eta}_{\mathrm{au}} = \left(\sum_{i=1}^{N_{\mathrm{u}}}\frac{\partial \eta_{\mathrm{au}}}{\partial q_i}\dot{q}_i\right) + \left(\sum_{k=1}^{N_{\mathrm{a}}}\frac{\partial \eta_{\mathrm{au}}}{\partial q_{ak}}\dot{q}_{ak}\right), \tag{13}$$

where

$$\frac{\partial \eta_{\mathrm{au}}}{\partial q_i} = \frac{\partial \eta_{\mathrm{au}}}{\partial d_{\mathrm{au}}}E_{\mathrm{au}}^{\mathrm{T}}\frac{\partial q_{\mathrm{u}}}{\partial q_i} + \frac{\partial \eta_{\mathrm{au}}}{\partial \Omega_{\mathrm{au}}}\frac{\partial \Omega_{\mathrm{au}}}{\partial R_{\mathrm{u}}}\frac{\partial R_{\mathrm{u}}}{\partial q_i},$$
$$\frac{\partial \eta_{\mathrm{au}}}{\partial q_{ak}} = \frac{\partial \eta_{\mathrm{au}}}{\partial \Omega_{\mathrm{au}}}\frac{\partial \Omega_{\mathrm{au}}}{\partial R_{\mathrm{a}}}\frac{\partial R_{\mathrm{a}}}{\partial q_{ak}} - \frac{\partial \eta_{\mathrm{au}}}{\partial d_{\mathrm{au}}}E_{\mathrm{au}}^{\mathrm{T}}\frac{\partial q_{\mathrm{a}}}{\partial q_{ak}}.$$

Next, let $E_{ti} \triangleq \frac{q_t - q_i}{d_{ti}} \in \mathbb{S}^2$, $\dot{\eta}_{ti}$ in (11) can be expressed as

$$\dot{\eta}_{ti} = \frac{\partial \eta_{ti}}{\partial d_{ti}} E_{ti}^{\mathrm{T}} (\dot{q}_t - \dot{q}_i) = \frac{\partial \eta_{ti}}{\partial q_i} \dot{q}_i + \frac{\partial \eta_{ti}}{\partial q_t} \dot{q}_t, \tag{14}$$

where

$$\frac{\partial \eta_{ti}}{\partial q_i} = -\frac{\partial \eta_{ti}}{\partial d_{ti}} E_{ti}^{\mathrm{T}}, \quad \frac{\partial \eta_{ti}}{\partial q_t} = \frac{\partial \eta_{ti}}{\partial d_{ti}} E_{ti}^{\mathrm{T}}.$$

Finally, let $E_{dij} \triangleq \frac{q_i - q_j}{\|q_i - q_j\|} \in \mathbb{S}^2$, $E_{ai} \triangleq \frac{q_i - q_a}{d_{ai}} \in \mathbb{S}^2$, $E_{aj} \triangleq \frac{q_j - q_a}{d_{aj}} \in \mathbb{S}^2$. $\dot{\eta}_{eij}$ in (11) yields

$$\dot{\eta}_{eij} = \frac{\partial \eta_{eij}}{\partial q_i} \dot{q}_i + \frac{\partial \eta_{eij}}{\partial q_j} \dot{q}_j + \sum_{k=1}^{N_a} \left(\frac{\partial \eta_{eij}}{\partial d_{ai}} \frac{\partial d_{ai}}{\partial q_{ak}} + \frac{\partial \eta_{eij}}{\partial d_{aj}} \frac{\partial d_{aj}}{\partial q_{ak}} \right) \dot{q}_{ak}, \tag{15}$$

where

$$\begin{aligned}
\frac{\partial \eta_{eij}}{\partial q_i} &= \Big(\frac{\partial \eta_{eij}}{\partial \Omega_{eHij}} \frac{\partial \Omega_{eHij}}{\partial d_{ai}} + \frac{\partial \eta_{eij}}{\partial \Omega_{eLij}} \frac{\partial \Omega_{eLij}}{\partial d_{ai}} \\
&\quad - \frac{\partial \eta_{eij}}{\partial d_{eij}} \frac{\partial d_{dij}}{\partial d_{ai}} \Big) E_{ai}^{\mathrm{T}} + \frac{\partial \eta_{eij}}{\partial d_{eij}} E_{dij}^{\mathrm{T}}, \\
\frac{\partial \eta_{eij}}{\partial q_j} &= \Big(\frac{\partial \eta_{eij}}{\partial \Omega_{eHij}} \frac{\partial \Omega_{eHij}}{\partial d_{aj}} + \frac{\partial \eta_{eij}}{\partial \Omega_{eLij}} \frac{\partial \Omega_{eLij}}{\partial d_{aj}} \\
&\quad - \frac{\partial \eta_{eij}}{\partial d_{eij}} \frac{\partial d_{dij}}{\partial d_{aj}} \Big) E_{aj}^{\mathrm{T}} - \frac{\partial \eta_{eij}}{\partial d_{eij}} E_{dij}^{\mathrm{T}}, \\
\frac{\partial \eta_{eij}}{\partial d_{ai}} \frac{\partial d_{ai}}{\partial q_{ak}} &= \Big(\frac{\partial \eta_{eij}}{\partial d_{eij}} \frac{\partial d_{dij}}{\partial d_{ai}} - \frac{\partial \eta_{eij}}{\partial \Omega_{eHij}} \frac{\partial \Omega_{eHij}}{\partial d_{ai}} \\
&\quad - \frac{\partial \eta_{eij}}{\partial \Omega_{eLij}} \frac{\partial \Omega_{eLij}}{\partial d_{ai}} \Big) \left(\frac{\partial R_a}{\partial q_{ak}} + E_{ai}^{\mathrm{T}} \frac{\partial q_a}{\partial q_{ak}} \right), \\
\frac{\partial \eta_{eij}}{\partial d_{aj}} \frac{\partial d_{aj}}{\partial q_{ak}} &= \Big(\frac{\partial \eta_{eij}}{\partial d_{eij}} \frac{\partial d_{dij}}{\partial d_{aj}} - \frac{\partial \eta_{eij}}{\partial \Omega_{eHij}} \frac{\partial \Omega_{eHij}}{\partial d_{aj}} \\
&\quad - \frac{\partial \eta_{eij}}{\partial \Omega_{eLij}} \frac{\partial \Omega_{eLij}}{\partial d_{aj}} \Big) \left(\frac{\partial R_a}{\partial q_{ak}} + E_{aj}^{\mathrm{T}} \frac{\partial q_a}{\partial q_{ak}} \right).
\end{aligned}$$

Now, we substitute $\dot{\Pi}_{tc}$ in (12), $\dot{\eta}_{ti}$ in (14), $\dot{\eta}_{au}$ in (13), and $\dot{\eta}_{eij}$ in (15) back into (11), which yields

$$\dot{V}_q = \sum_{i=1}^{N_u} \left(\frac{\partial V_q}{\partial q_i} \dot{q}_i + G_{ti}^{\mathrm{T}} \dot{q}_t + g_{tc} \dot{\omega}_{tc} + \sum_{k=1}^{N_a} G_{aik}^{\mathrm{T}} \dot{q}_{ak} \right), \tag{16}$$

where

$$\begin{aligned}
\frac{\partial V_q}{\partial q_i} &= \frac{\partial \Pi_{tc}}{\partial q_i} + \eta_{au} \frac{\partial \eta_{au}}{\partial q_i} + \eta_{ti} \frac{\partial \eta_{ti}}{\partial q_i} + \sum_{j=1, j \neq i}^{N_u} 2 \eta_{eij} \frac{\partial \eta_{eij}}{\partial q_i}, \\
G_{ti} &\triangleq \frac{1}{N_u} \left(\frac{\partial \Pi_{tc}}{\partial q_t} \right)^{\mathrm{T}} + \eta_{ti} \left(\frac{\partial \eta_{ti}}{\partial q_t} \right)^{\mathrm{T}}, \quad g_{tc} \triangleq \frac{1}{N_u} \frac{\partial \Pi_{tc}}{\partial \omega_{tc}}, \\
G_{aik} &\triangleq \frac{1}{N_u} \left(\frac{\partial \Pi_{tc}}{\partial q_{ak}} \right)^{\mathrm{T}} + \frac{1}{N_u} \eta_{au} \left(\frac{\partial \eta_{au}}{\partial q_{ak}} \right)^{\mathrm{T}} \\
&\quad + \sum_{j=1, j \neq i}^{N_u} 2 \eta_{eij} \left(\frac{\partial \eta_{eij}}{\partial d_{ai}} \frac{\partial d_{ai}}{\partial q_{ak}} \right)^{\mathrm{T}}.
\end{aligned}$$

By using (1) and Assumption 1, the term $\frac{\partial V_q}{\partial q_i} \dot{q}_i$ in (16) is written as

$$\frac{\partial V_q}{\partial q_i} \dot{q}_i = \frac{\partial V_q}{\partial q_i} (p_i + \xi_i) \leq \frac{\partial V_q}{\partial q_i} p_i + \left\| \frac{\partial V_q}{\partial q_i} \right\| \bar{\xi}_i, \tag{17}$$

where $\bar{\xi}_i$ is the unknown bound for external disturbance ξ_i introduced in Assumption 1.

Furthermore, under Assumption 3 and Lemma 1, the term $G_{ti}^{\mathrm{T}} \dot{q}_t$ in (16) can be expressed as

$$\begin{aligned}
G_{ti}^{\mathrm{T}} \dot{q}_t &= G_{ti}^{\mathrm{T}} p_t = G_{ti}^{\mathrm{T}} \left(W_t^{\mathrm{T}} B_t + \epsilon_t \right) \\
&= G_{ti}^{\mathrm{T}} \left[W_t^{\mathrm{T}} B_{ti} + W_t^{\mathrm{T}} (B_t - B_{ti}) + \epsilon_t \right] \\
&= (B_{ti} \otimes G_{ti})^{\mathrm{T}} \mathrm{vec}(W_t^{\mathrm{T}}) + G_{ti}^{\mathrm{T}} \left[W_t^{\mathrm{T}} (B_t - B_{ti}) + \epsilon_t \right] \\
&\leq (B_{ti} \otimes G_{ti})^{\mathrm{T}} w_t + \|G_{ti}\| (\|W_t\| \sqrt{\gamma} + \bar{\epsilon}_t),
\end{aligned} \tag{18}$$

where $B_{ti} \triangleq B_t(\mathcal{X}_{ti})$ with $\mathcal{X}_{ti} = q_t - q_i \in \mathbb{R}^3$, and $w_t \triangleq \mathrm{vec}(W_t^{\mathrm{T}}) \in \mathbb{R}^{3\gamma}$.

Moreover, under Assumption 4 and Lemma 1, the term $G_{aik}^{\mathrm{T}} \dot{q}_{ak}$ in (16) can be rewritten as

$$\begin{aligned}
G_{aik}^{\mathrm{T}} \dot{q}_{ak} &= G_{aik}^{\mathrm{T}} p_{ak} = G_{aik}^{\mathrm{T}} \left(W_{ak}^{\mathrm{T}} B_{ak} + \epsilon_{ak} \right) \\
&= G_{aik}^{\mathrm{T}} \left[W_{ak}^{\mathrm{T}} B_{aik} + W_{ak}^{\mathrm{T}} (B_{ak} - B_{aik}) + \epsilon_{ak} \right] \\
&= (B_{aik} \otimes G_{aik})^{\mathrm{T}} \mathrm{vec}(W_{ak}^{\mathrm{T}}) \\
&\quad + G_{aik}^{\mathrm{T}} \left[W_{ak}^{\mathrm{T}} (B_{ak} - B_{aik}) + \epsilon_{ak} \right] \\
&\leq (B_{aik} \otimes G_{aik})^{\mathrm{T}} w_{ak} + \|G_{aik}\| (\|W_{ak}\| \sqrt{\gamma} + \bar{\epsilon}_{ak}),
\end{aligned} \tag{19}$$

where $B_{aik} \triangleq B_{ak}(\mathcal{X}_{aik})$ with $\mathcal{X}_{aik} = q_i - q_{ak} \in \mathbb{R}^3$, and $w_{ak} \triangleq \mathrm{vec}(W_{ak}^{\mathrm{T}}) \in \mathbb{R}^{3\gamma}$.

Next, taking (17)–(19) into (16), $\dot{V}_q$ yields

$$\dot{V}_q \leq \sum_{i=1}^{N_u} \left(\frac{\partial V_q}{\partial q_i} p_i + g_{tc} \dot{\omega}_{tc} + G_{qi}^{\mathrm{T}} \delta_i \right), \tag{20}$$

where

$$\begin{aligned}
G_{qi} &\triangleq [g_{\epsilon i}, \ (B_{ti} \otimes G_{ti})^{\mathrm{T}}, \ \underbrace{\cdots, \ (B_{aik} \otimes G_{aik})^{\mathrm{T}}, \ \cdots}_{k=1,\cdots,N_a}]^{\mathrm{T}}, \\
\delta_i &\triangleq [\bar{\epsilon}_i, \ w_t^{\mathrm{T}}, \ \underbrace{\cdots, \ w_{ak}^{\mathrm{T}}, \ \cdots}_{k=1,\cdots,N_a}]^{\mathrm{T}},
\end{aligned}$$

in which $G_{qi} \in \mathbb{R}^{3\gamma(N_a+1)+1}$, $\delta_i \in \mathbb{R}^{3\gamma(N_a+1)+1}$, $g_{\epsilon i} \triangleq \left\| \frac{\partial V_q}{\partial q_i} \right\| + \|G_{ti}\| + \sum_{k=1}^{N_a} \|G_{aik}\|$, and $\bar{\epsilon}_i \triangleq \max_{k=1,\cdots,N_a} \left\{ \bar{\xi}_i, \ \|W_t\| \sqrt{\gamma} + \bar{\epsilon}_t, \ \|W_{ak}\| \sqrt{\gamma} + \bar{\epsilon}_{ak} \right\}$. Note that δ_i is an unknown constant vector.

Now, consider $V_p = \sum_{i=1}^{N_u} \frac{1}{2} p_i^{\mathrm{T}} p_i$. Let $V_{qp} = V_q + V_p$, from (20) we have

$$\dot{V}_{qp} \leq \sum_{i=1}^{N_u} \left\{ p_i^{\mathrm{T}} \left[\left(\frac{\partial V_q}{\partial q_i} \right)^{\mathrm{T}} + \dot{p}_i \right] + g_{tc} \dot{\omega}_{tc} + G_{qi}^{\mathrm{T}} \delta_i \right\}, \tag{21}$$

For the ith agent, the control law $p_i \in \mathbb{R}^3$ is designed as

$$\begin{aligned}
\dot{p}_i &= -K_{pi} p_i - \left(\frac{\partial V_q}{\partial q_i} \right)^{\mathrm{T}} - \frac{p_i}{p_i^{\mathrm{T}} p_i} \Big(g_{tc} \dot{\omega}_{tc} + G_{qi}^{\mathrm{T}} \hat{\delta}_i + K_{ti} \eta_{ti}^2 \\
&\quad + \frac{1}{N_u} K_{tc} \Pi_{tc} + \frac{1}{N_u} K_{au} \eta_{au}^2 + \sum_{j=1, j \neq i}^{N_u} K_{eij} \eta_{eij}^2 \Big), \\
p_i &= \int_0^t \dot{p}_i \mathrm{d}\tau + p_{i0},
\end{aligned} \tag{22}$$

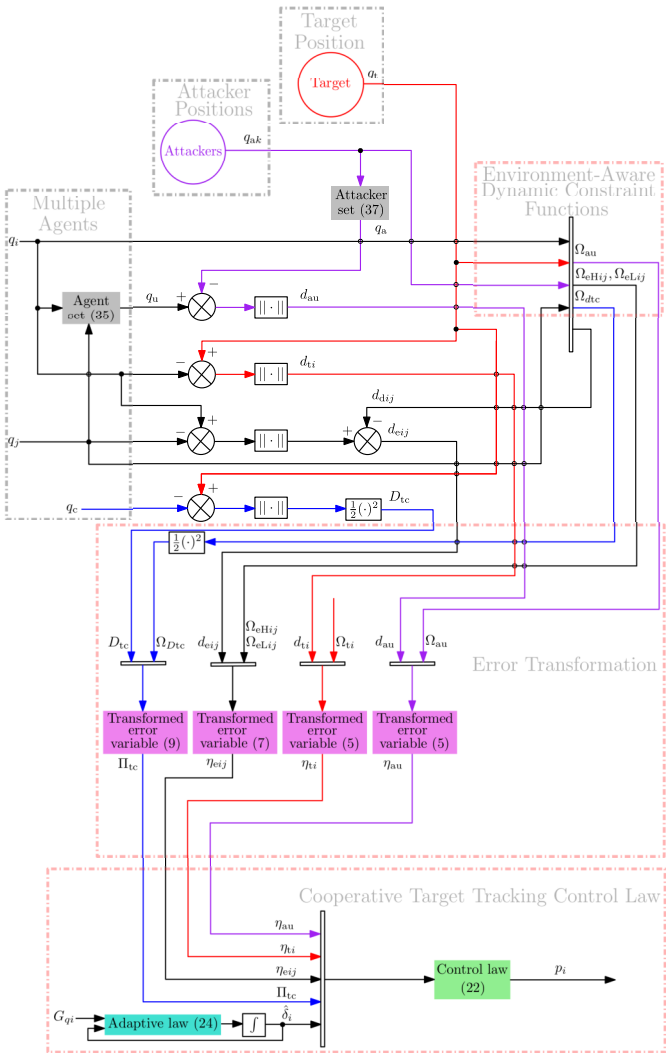

Fig. 7. Block diagram of the overall control algorithm.

where $K_{pi} > 0$, $K_{ti} > 0$, $K_{tc} > 0$, $K_{au} > 0$, and $K_{eij} > 0$. $p_{i0} \in \mathbb{R}^3$, $\|p_{i0}\| > 0$ is the initial velocity. $\hat{\delta}_i$ is the estimation of δ_i introduced in (20).

Substituting the control law designed in (22) back into (21) yields

$$\dot{V}_{qp} \le \sum_{i=1}^{N_u} \left(-K_{ti}\eta_{ti}^2 - \sum_{j=1, j\neq i}^{N_u} K_{eij}\eta_{eij}^2 - K_{pi}p_i^{\mathrm{T}}p_i - G_{qi}^{\mathrm{T}}\tilde{\delta}_i \right) - K_{tc}\Pi_{tc} - K_{au}\eta_{au}^2, \tag{23}$$

where $\tilde{\delta}_i \triangleq \hat{\delta}_i - \delta_i$, with the adaptive law for the estimator $\hat{\delta}_i$ designed as

$$\dot{\hat{\delta}}_i = n_{\delta i}G_{qi} - \sigma_{\delta i}\hat{\delta}_i, \tag{24}$$

where $\hat{\delta}_i(0) = \hat{\delta}_{i0}$ with $\hat{\delta}_{i0}$ being the initial condition, $n_{\delta i} > 0$, and $\sigma_{\delta i} > 0$.

Now, let $V_\delta = \sum_{i=1}^{N_u} \frac{1}{2n_{\delta i}}\tilde{\delta}_i^{\mathrm{T}}\tilde{\delta}_i$, denote $V_{\mathrm{MAS}} = V_{qp} + V_\delta$. For the time derivative of V_{MAS} we can get

$$\dot{V}_{\mathrm{MAS}} \le -\kappa_1 V_{\mathrm{MAS}} + \varrho_1, \tag{25}$$

where $\kappa_1 \triangleq \min_{i,j=1,\cdots,N_u,\ j\neq i}\{K_{tc},\ 2K_{au},\ 2K_{ti},\ 2K_{eij}, 2K_{pi},\ \sigma_{\delta i}\}$ and $\varrho_1 \triangleq \sum_{i=1}^{N_u} \frac{\sigma_{\delta i}}{2n_{\delta i}}\delta_i^{\mathrm{T}}\delta_i$. The overall control algorithm can be summarized into the block diagram shown in Figure 7.

The aforementioned design procedure leads to the following theoretical result.

Theorem 1: With the control laws (22), and adaptive laws (24), the multi-agent system described by (1) under Assumptions 1-5 will have following results:

1) The constraint requirements in (CO1)-(CO4) are met.
2) The target fencing error $\|q_c - q_t\|$ is confined in the range (26), as shown at the bottom of the next page, for all time.
3) The transformed relative distance tracking error η_{eij} will converge into the following set as $t \to \infty$

$$\left\{ \eta_{eij} \;\middle|\; |\eta_{eij}| \le \varepsilon_e, \quad \varepsilon_e \triangleq \sqrt{\frac{2\varrho_1}{\kappa_1}} \right\}, \tag{27}$$

which implies that relative distance tracking errors d_{eij} will converge into the following region

$$\left\{ d_{eij} \mid -\varepsilon_{eLij} \le d_{eij} \le \varepsilon_{eHij} \right\}, \tag{28}$$

where ε_{eHij} and ε_{eLij} are expressed as

$$\varepsilon_{eHij} \triangleq \frac{\left(\begin{array}{c} -\left(\Omega_{eHij}\Omega_{eLij} - \varepsilon_e\left(\Omega_{eHij} - \Omega_{eLij}\right)\right) \\ + \sqrt{\begin{array}{c}\Omega_{eHij}^2\Omega_{eLij}^2 + \varepsilon_e^2\left(\Omega_{eHij} + \Omega_{eLij}\right)^2 \\ -2\varepsilon_e\Omega_{eHij}\Omega_{eLij}\left(\Omega_{eHij} - \Omega_{eLij}\right)\end{array}} \end{array} \right)}{2\varepsilon_e},$$

$$\varepsilon_{eLij} \triangleq \frac{\left(\begin{array}{c} -\left(\Omega_{eHij}\Omega_{eLij} + \varepsilon_e\left(\Omega_{eHij} - \Omega_{eLij}\right)\right) \\ + \sqrt{\begin{array}{c}\Omega_{eHij}^2\Omega_{eLij}^2 + \varepsilon_e^2\left(\Omega_{eHij} + \Omega_{eLij}\right)^2 \\ +2\varepsilon_e\Omega_{eHij}\Omega_{eLij}\left(\Omega_{eHij} - \Omega_{eLij}\right)\end{array}} \end{array} \right)}{2\varepsilon_e},$$

hence (CO5) is met.

4) The control laws (22) and adaptive laws (24) are all uniformly bounded.

Proof: From (25), for $t \ge 0$ we have

$$V_{\mathrm{MAS}}(t) \le \left(V_{\mathrm{MAS0}} - \frac{\varrho_1}{\kappa_1} \right) \exp(-\kappa_1 t) + \frac{\varrho_1}{\kappa_1}, \tag{29}$$

where V_{MAS0} is the initial value of $V_{\mathrm{MAS}}(t)$. The inequality in (29) implies that $V_{\mathrm{MAS}}(t) \le \bar{V}_{\mathrm{MAS}}$, $\forall t \ge 0$, where $\bar{V}_{\mathrm{MAS}} \triangleq V_{\mathrm{MAS0}} + \frac{\varrho_1}{\kappa_1}$. The uniform boundedness of V_{MAS} implies boundedness of Π_{tc} (defined in (9)), η_{au}, η_{ti} (defined in (5)), and η_{eij} (defined in (7)). Moreover, boundedness of η_{au} and η_{ti} implies (CO1) and (CO2) are met, and boundedness of η_{eij} implies that $-\Omega_{eLij} < d_{eij} < \Omega_{eHij}$, which implies that (CO3) is achieved. Last but not least, boundedness of Π_{tc} implies $D_{tc} < \Omega_{Dtc}$, which implies (CO4) is met.

Next, since (CO1) is met, Proposition 1 holds true. Furthermore, since (CO3) is met, the target fencing error is confined in the range (26).

Moreover, from (25) we have $\limsup_{t\to\infty} V_{\mathrm{MAS}} \le \frac{\varrho_1}{\kappa_1}$, hence $\limsup_{t\to\infty} |\eta_{eij}| \le \sqrt{\frac{2\varrho_1}{\kappa_1}}$, therefore η_{eij} will converge to the set (27) as time evolves.

Note that the range in (28) can be arbitrarily small (Details can be seen in Remarks 9 and 10). Thus, (CO5) can be achieved with the proposed control framework. Now, recall that $\eta_{eij} = \frac{\Omega_{\mathrm{eH}ij}\Omega_{\mathrm{eL}ij}d_{eij}}{(\Omega_{\mathrm{eH}ij}-d_{eij})(\Omega_{\mathrm{eL}ij}+d_{eij})}$, the set in (27) implies the set (28).

Finally, uniform boundedness of V_{MAS} implies boundedness of adaptive estimates $\hat{\delta}_i$ in (22), and variables G_{qi} in (20). Moreover, adaptive laws $\dot{\hat{\delta}}_i$ in (24) are also uniformly bounded due to the boundedness of $\hat{\delta}_i$ in (22) and G_{qi} in (20). ■

Remark 9: In Theorem 1, using L'Hôpital's rule yields

$$\lim_{\varepsilon_{\mathrm{e}}\to 0}\varepsilon_{\mathrm{eH}ij}=0,\quad \lim_{\varepsilon_{\mathrm{e}}\to 0}\varepsilon_{\mathrm{eL}ij}=0. \tag{30}$$

This implies that when the transformed error variable η_{eij} converges into a small neighborhood of zero, the relative distance tracking error d_{eij} can converge to a region close to zero.

Remark 10: To reduce the set size in (27), we need to select large κ_1 and small ϱ_1. To make κ_1 large, we can select large control gains K_{tc}, K_{au}, $K_{\mathrm{t}i}$, K_{eij}, and K_{pi}, and large adaptive parameter $\sigma_{\delta i}$. To make ϱ_1 small, we can select large adaptive parameters $n_{\delta i}$.

V. Simulation Studies

In this section, we conduct simulations with a team of $N_{\mathrm{u}}=4$ agents in the presence of $N_{\mathrm{a}}=3$ physical attackers. Units for position and velocity are m and m/s, respectively. The initial positions of the agents, target, and attackers are $q_{10}=[0.5,\ 2.5,\ 1]^{\mathrm{T}}$, $q_{20}=[0.5,\ 0.5,\ -1]^{\mathrm{T}}$, $q_{30}=[2.5,\ -0.5,\ 2]^{\mathrm{T}}$, $q_{40}=[2.5,\ 2.5,\ -2]^{\mathrm{T}}$, $q_{\mathrm{t}0}=[5,\ 5,\ 12]^{\mathrm{T}}$, $q_{\mathrm{a}10}=[5,\ 15,\ 55]^{\mathrm{T}}$, $q_{\mathrm{a}20}=[-5,\ 12,\ 55]^{\mathrm{T}}$, and $q_{\mathrm{a}30}=[0,\ 11,\ 105]^{\mathrm{T}}$. Besides, the ith agent's ($i=1,2,3,4$) initial velocity is $p_{i0}=[1,\ 1,\ -1]^{\mathrm{T}}$. Moreover, the unknown disturbances for agents are $\xi_i=[0.105\sin(0.2t),\ 0.25\cos(0.2t),\ 0.3\cos(0.15t)]^{\mathrm{T}}$, $i=1,2,3,4$.

The number of neural network nodes is chosen as $\gamma=4$. Basis functions in the Subsection IV-A are given as $b_l=\exp\left[-\frac{(\mathcal{X}_{ti}-\nu_l)^{\mathrm{T}}(\mathcal{X}_{ti}-\nu_l)}{\zeta_l^2}\right]$ and $b_{kl}=\exp\left[-\frac{(\mathcal{X}_{aik}-\nu_{kl})^{\mathrm{T}}(\mathcal{X}_{aik}-\nu_{kl})}{\zeta_{kl}^2}\right]$, where $i=1,2,3,4$ is the index of agents, $k=1,2,3$ represents the index of attackers, and $l=1,2,3,4$ corresponds to the index of neural network nodes. For these basis functions, the width values are given as $\zeta_1=\zeta_{k1}=2$, $\zeta_2=\zeta_{k2}=1$, $\zeta_3=\zeta_{k3}=0.5$, and $\zeta_4=\zeta_{k4}=0.25$. The receptive field's centers are selected as $\nu_1=\nu_{k1}=20\cdot\mathbf{1}_3$, $\nu_2=\nu_{k2}=10\cdot\mathbf{1}_3$, $\nu_3=\nu_{k3}=-10\cdot\mathbf{1}_3$, and $\nu_4=\nu_{k4}=-20\cdot\mathbf{1}_3$, where $\mathbf{1}_3\triangleq[1,\ 1,\ 1]^{\mathrm{T}}$ and $k=1,2,3$. The control gains and design parameters are chosen as $K_{\mathrm{tc}}=0.45$, $K_{\mathrm{au}}=0.75$, $K_{\mathrm{t}i}=0.05$, $K_{eij}=0.75$, $K_{pi}=0.075$, $n_{\delta i}=3.5$, and $\sigma_{\delta i}=0.35$, where $i,j=1,2,3,4$, $j\neq i$.

For safety constraints, we select $\Omega_{\mathrm{a}}=2.5$ in (CO1), and $\Omega_{\mathrm{t}i}=1.5$ ($i=1,2,3,4$) in (CO2). As shown in Remark 6, for (CO3) and (CO5) we design $\Omega_{\mathrm{H}ij}=\bar{\Omega}_{ij}-0.5t[\exp(-\alpha_{ij}d_{\mathrm{a}i})+\exp(-\alpha_{ij}d_{\mathrm{a}j})]$, $\Omega_{\mathrm{L}ij}=\underline{\Omega}_{ij}+0.5t[\exp(-\alpha_{ij}d_{\mathrm{a}i})+\exp(-\alpha_{ij}d_{\mathrm{a}j})]$, and $d_{\mathrm{d}ij}=l_{\mathrm{d}ij}+0.5\ l_{\mathrm{d}ij}(\lambda_{ij}-1)\Big[\exp\big(-\alpha_{ij}(d_{\mathrm{a}i}-\Omega_{\mathrm{a}})\big)+\exp(-\alpha_{ij}(d_{\mathrm{a}j}-\Omega_{\mathrm{a}}))\Big]$ where $\bar{\Omega}_{ij}=5.05\exp(-0.15t)+14.45$, $\underline{\Omega}_{ij}=12.5\exp(-0.25t)+14.5$, $\iota=6.3$, $\alpha_{ij}=0.1$, $l_{\mathrm{d}ij}=14$, and $\lambda_{ij}=0.55$. Additionally, for (CO4) we design $\Omega_{d\mathrm{tc}}=\mathrm{softmax}_{\rho_{\mathrm{tc}}}\big(R_{\mathrm{a}}+\Omega_{\mathrm{a}}-\tanh(\|q_{\mathrm{t}}-q_{\mathrm{a}}\|)\|q_{\mathrm{t}}-q_{\mathrm{a}}\|+\mu_{\mathrm{tc}},\ \omega_{\mathrm{tc}}\big)$ where $\mu_{\mathrm{tc}}=15$, $\rho_{\mathrm{tc}}=1$, and $\omega_{\mathrm{tc}}=34.4\exp(-0.6t)+0.6$.

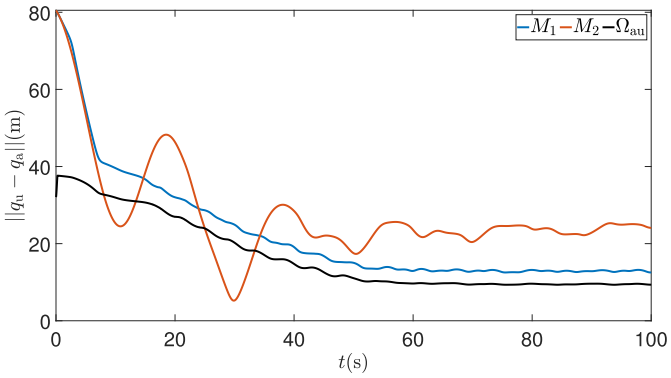

Fig. 8. The distance between center of agent set q_{u} and center of attacker set q_{a} under M_1 and M_2 with safety constraint $\Omega_{\mathrm{au}}\triangleq R_{\mathrm{u}}+R_{\mathrm{a}}+\Omega_{\mathrm{a}}$.

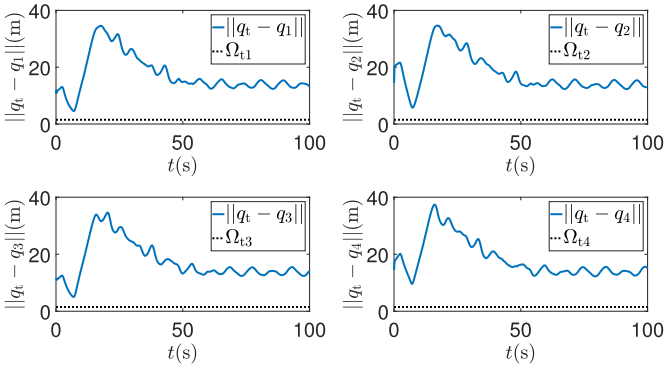

Fig. 9. The distance between each agent and the target $\|q_{\mathrm{t}}-q_i\|$ and safety constraint $\Omega_{\mathrm{t}i}$.

We consider two simulation scenarios:

(1) Persistent attacks: attackers consistently disrupt agents;

(2) Temporary attacks: attackers disrupt agents for a limited time before retreating.

In both simulation scenarios, the target's velocity is $p_{\mathrm{t}}=\mathrm{sat}(u_{\mathrm{t}})$, $u_{\mathrm{t}}=p_{\mathrm{c}}-K_{\mathrm{t}}(q_{\mathrm{c}}-q_{\mathrm{t}})$, which is unknown to agents, where the saturation bound is $\bar{p}_{\mathrm{t}}=2.5$ and $K_{\mathrm{t}}=500$.

In order to show the effectiveness of our proposed control framework, we conduct a comparative study with a cooperative target tracking controller [23] which only considers constant constraint requirements for vehicles. This controller is $p_i=\phi_i+k_1(q_{\mathrm{t}}-q_i)+v_i$ where $\dot{v}_i=k_2(q_{\mathrm{t}}-q_i)$, $\phi_i=\frac{1}{\|q_{\mathrm{t}}-q_i\|-1.5}+\sum_{j=1,j\neq i}^{4}\left(\frac{1}{\|q_i-q_j\|-0.55}+\frac{1}{25-\|q_i-q_j\|}\right)+\sum_{k=1}^{3}\left(\frac{1}{\|q_i-q_{ak}\|-2.5}\right)$, $k_1=$

$$\Big\{\|q_{\mathrm{c}}-q_{\mathrm{t}}\|\ \Big|\ 0\le\|q_{\mathrm{c}}-q_{\mathrm{t}}\|<\Omega_{d\mathrm{tc}},\quad \text{when } R_{\mathrm{a}}+\Omega_{\mathrm{a}}-\|q_{\mathrm{t}}-q_{\mathrm{a}}\|<0;$$
$$R_{\mathrm{a}}+\Omega_{\mathrm{a}}-\|q_{\mathrm{t}}-q_{\mathrm{a}}\|<\|q_{\mathrm{c}}-q_{\mathrm{t}}\|<\Omega_{d\mathrm{tc}},\ \text{when } R_{\mathrm{a}}+\Omega_{\mathrm{a}}-\|q_{\mathrm{t}}-q_{\mathrm{a}}\|\ge 0\Big\}. \tag{26}$$

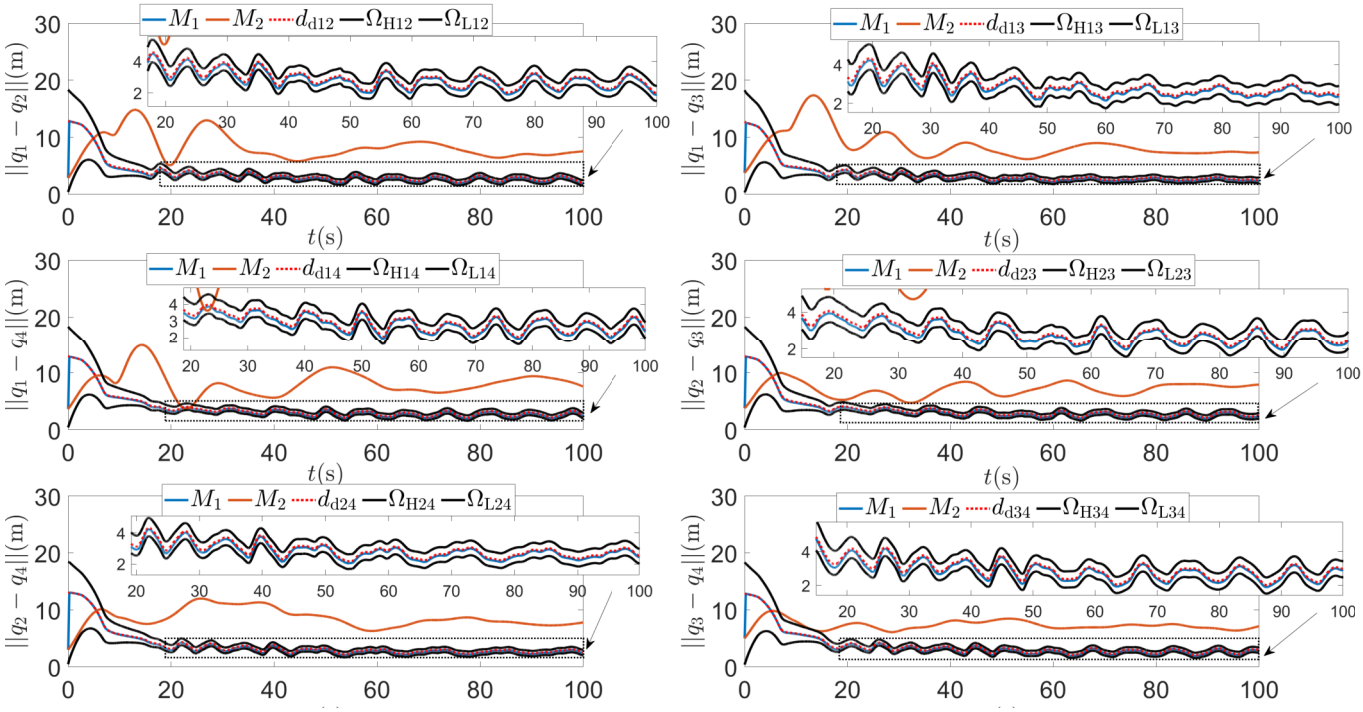

Fig. 10. Relative distance between the ith and jth agents $\|q_i - q_j\|$ under M_1 and M_2 with its desired signal d_{dij} and safety constraint functions Ω_{Hij} and Ω_{Lij}.

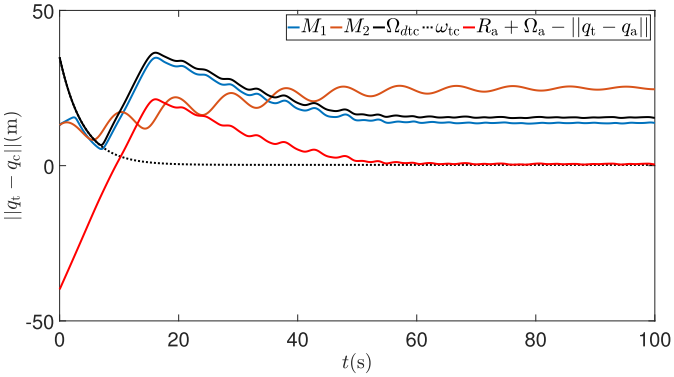

Fig. 11. The target tracking error $\|q_t - q_c\|$ under M_1 and M_2 with its constraint functions.

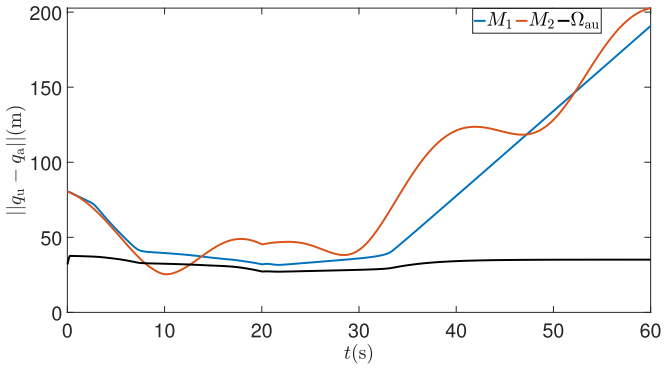

Fig. 12. The distance between center of agent set q_u and center of attacker set q_a under M_1 and M_2 with safety constraint $\Omega_{au} \triangleq R_u + R_a + \Omega_a$.

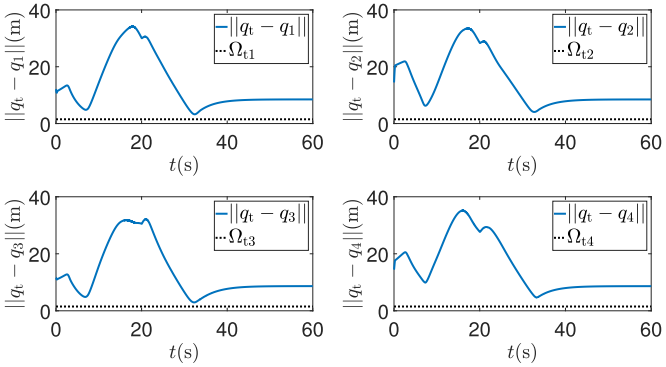

Fig. 13. The distance between each agent and the target $\|q_t - q_i\|$ and safety constraint Ω_{ti}.

$k_2 = 0.45$, and $i = 1, 2, 3, 4$. Besides, initial states of the target, attackers, and agents are identical for both controllers. For simplicity of expression, we denote our proposed controller as M_1, and the controller designed in [23] as M_2 in the following discussion.

A. Scenario 1: Persistent Attacks

In this scenario, multiple attackers continuously launch physical attacks on agents. The kth attacker's velocity ($k = 1, 2, 3$) is $p_{ak} = \text{sat}(u_{ak})$, $u_{ak} = p_k - K_{ak}(q_{ak} - q_k)$, which is unknown to agents, where the saturation bound is $\bar{p}_{ak} = 2$ and $K_{ak} = 1300$. Simulation results are presented in Figures 8–11. A YouTube video for the simulation process can also be viewed at: https://youtu.be/zF4isCd-sQw (To view the video, copy and paste the complete URL to a web browser).

Specifically, Figure 8 shows the distance between center of agent set q_u and center of attacker set q_a, alongside with $\Omega_{au} \triangleq R_u + R_a + \Omega_a$ under M_1 and M_2. Under M_1, $\|q_u -$

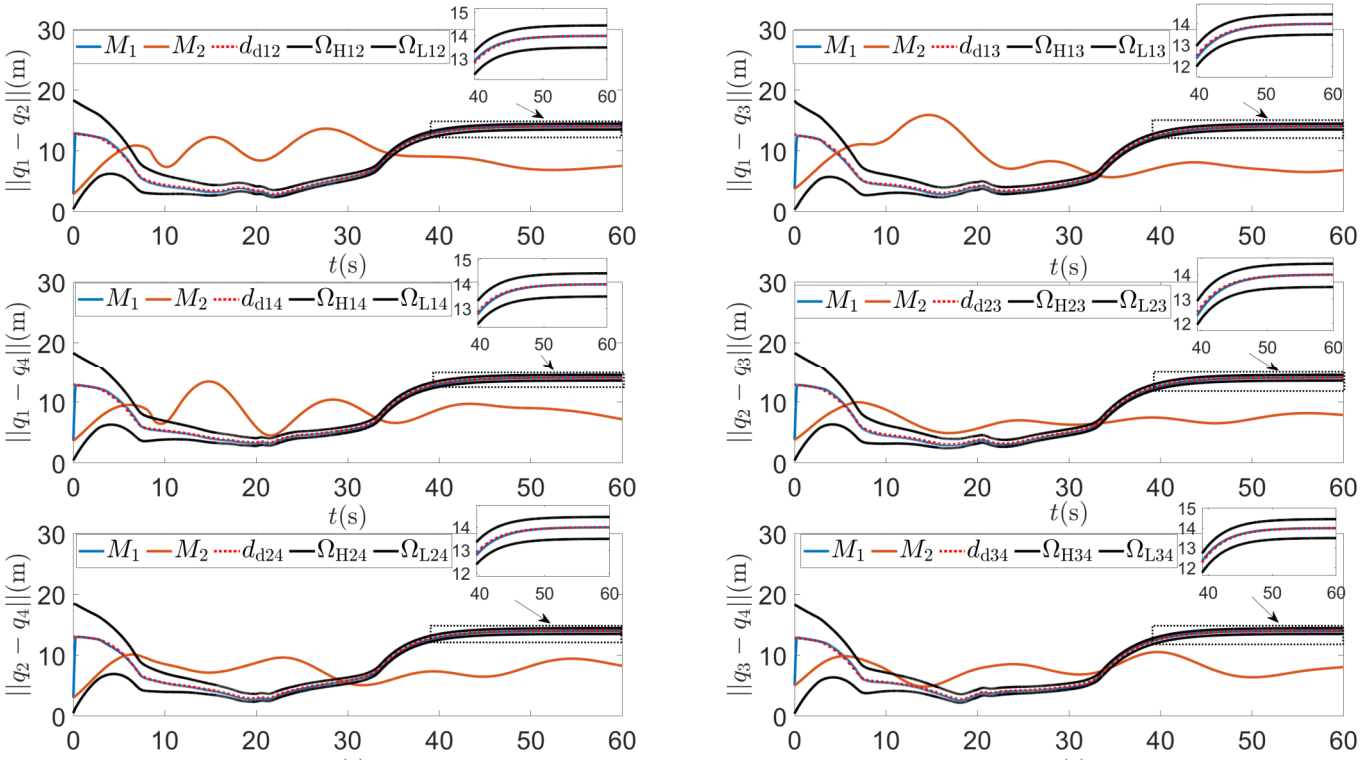

Fig. 14. Relative distance between the ith and jth agents $\|q_i - q_j\|$ under M_1 and M_2 with its desired signal d_{dij} and safety constraint functions Ω_{Hij} and Ω_{Lij}.

$q_a\|$ remains larger than Ω_{au}, indicating that (CO1) is met. In contrast, under M_2, the safety constraint in (CO1) is violated during the intervals $8 \le t \le 14$ and $24 \le t \le 33$. Next, Figure 9 presents the distance between the ith agent ($i = 1, 2, 3, 4$) and target $\|q_t - q_i\|$, with safety constraint Ω_{ti}. Since $\|q_t - q_i\|$ stays above Ω_{ti}, (CO2) is guaranteed.

Moreover, Figure 10 illustrates the relative distance between the ith and jth agents $\|q_i - q_j\|$, the desired inter-agent distance d_{dij}, and safety constraint functions Ω_{Hij} and Ω_{Lij} under M_1 and M_2, where $i, j = 1, 2, 3, 4$ and $j \ne i$. Under M_1, the relative distances $\|q_i - q_j\|$ can remain bounded between Ω_{Lij} and Ω_{Hij}, while converging to regions near the desired inter-agent distances d_{dij}. This demonstrates that (CO3) and (CO5) are satisfied. Note that d_{dij}, Ω_{Hij}, and Ω_{Lij} are *environment-aware and dynamic*, as discussed in Remark 6. More specifically, from Figure 10 we observe that d_{dij} decreases as attackers approach agents and increases as attackers move away. Additionally, Ω_{Hij} and Ω_{Lij} become tightened as attackers approach agents and are relaxed as attackers move away. Under M_2, the higher safety constraint requirements for relative distances are violated when $t \ge 7$, indicating (CO3) is not satisfied.

Besides, Figure 11 represents the target tracking error $\|q_t - q_c\|$, along with $R_a + \Omega_a - \|q_t - q_a\|$, performance constraint function Ω_{dtc}, and user-defined time-varying function ω_{tc} under M_1 and M_2. Under M_1, $\|q_t - q_c\|$ remains in the set defined by (26), hence (CO4) is met. More specifically, when attackers move close to the target, agents can no longer stay close to the target without violation of the safety constraint requirement $\|q_u - q_a\| > \Omega_{au}$. Since (CO1) has a higher priority than (CO4), Ω_{dtc} should be designed to ensure there is sufficient feasible space to maintain $\|q_u - q_a\| > \Omega_{au}$,

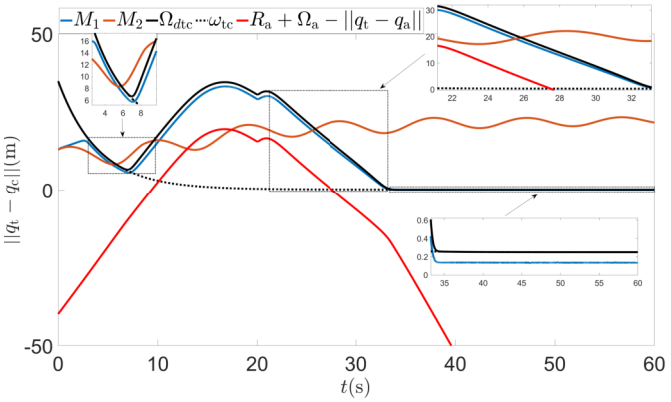

Fig. 15. The target tracking error $\|q_t - q_c\|$ under M_1 and M_2 with its constraint functions.

as discussed in Remarks 5 and 7. In contrast, under M_2, the performance constraint requirement in (CO4) is violated during the intervals $5 \le t \le 10$ and $t \ge 37$.

B. Scenario 2: Temporary Attacks

In this scenario, multiple attackers attempt to first launch physical attacks on agents, then leave the area. More specifically, when $t \le 20$, the kth attacker's velocity ($k = 1, 2, 3$) is chosen as $p_{ak} = \text{sat}(u_{ak})$, where $u_{ak} = p_k - K_{ak}(q_{ak} - q_k)$ with the upper bound $\bar{p}_{ak} = 2$ and $K_{ak} = 1300$. For $t > 20$, the kth attacker's velocity ($k = 1, 2, 3$) is chosen as $p_{ak} = p_{ak,20}\exp(-25(t-20)) + [1 - \exp(-25(t-20))] \cdot [2, 5, -2.5, 2.5]^T$ where $p_{ak,20}$ is the velocity of the kth attacker p_{ak} at $t = 20$. Simulation results are presented in Figures 12–15. A YouTube

video for the simulation process can also be viewed at: https://youtu.be/NpiW8eFdwn4 (To view the video, copy and paste the complete URL to a web browser).

Specifically, Figure 12 shows the distance between center of agent set $q_{\rm u}$ and center of attacker set $q_{\rm a}$, alongside with $\Omega_{\rm au} \triangleq R_{\rm u} + R_{\rm a} + \Omega_{\rm a}$ under M_1 and M_2. Under M_1, we see that $\|q_{\rm u} - q_{\rm a}\|$ is always above $\Omega_{\rm au}$, which implies (CO1) is ensured. In contrast, under M_2, the safety constraint requirement in (CO1) is violated when $8 \le t \le 13$. Furthermore, Figure 13 presents the distance between the ith agent ($i = 1, 2, 3, 4$) and target $\|q_{\rm t} - q_i\|$, with the safety constraint constant $\Omega_{{\rm t}i}$. Since $\|q_{\rm t} - q_i\|$ remains higher than $\Omega_{{\rm t}i}$, (CO2) is guaranteed. Moreover, Figure 14 records the relative distance between the ith and jth agents $\|q_i - q_j\|$, the desired inter-agent distance $d_{{\rm d}ij}$, and safety constraint functions $\Omega_{{\rm H}ij}$ and $\Omega_{{\rm L}ij}$ under M_1 and M_2, where $i, j = 1, 2, 3, 4$, $j \ne i$. Under M_1, $\|q_i - q_j\|$ is bounded by $\Omega_{{\rm H}ij}$ and $\Omega_{{\rm L}ij}$, and it converges to a region close to $d_{{\rm d}ij}$, indicating (CO3) and (CO5) are satisfied. Note that $d_{{\rm d}ij}$, $\Omega_{{\rm H}ij}$, and $\Omega_{{\rm L}ij}$ are *environment-aware and dynamic*, as discussed in Remark 6. On the one hand, we observe that $d_{{\rm d}ij}$ decreases and constraint functions $\Omega_{{\rm H}ij}$ and $\Omega_{{\rm L}ij}$ become tightened when attackers approach agents during $0 \le t \le 20$. On the other hand, when $t > 20$, $d_{{\rm d}ij}$ increase to $l_{{\rm d}ij}$, allowing the agents to maintain a relaxed formation. Under M_2, the higher safety constraints on relative distances are violated during $16 \le t \le 28$ and the lower safety constraints are violated for $t \ge 35$, which indicate that (CO3) is not satisfied.

Next, the target tracking error $\|q_{\rm t} - q_{\rm c}\|$, along with $R_{\rm a} + \Omega_{\rm a} - \|q_{\rm t} - q_{\rm a}\|$, the performance constraint function $\Omega_{d{\rm tc}}$, and user-defined time-varying function $\omega_{\rm tc}$ under M_1 and M_2, are presented in Figure 15. Under M_1, we can observe that $\|q_{\rm t} - q_{\rm c}\|$ remains in the set (26), which means (CO4) is achieved. More specifically, when attackers move close to the target, agents can no longer stay close to the target without violating the safety constraint requirement $\|q_{\rm u} - q_{\rm a}\| > \Omega_{\rm au}$. Similar to the first scenario, $\Omega_{d{\rm tc}}$ needs to be designed to ensure there is sufficient feasible space to maintain $\|q_{\rm u} - q_{\rm a}\| > \Omega_{\rm au}$. For $t \ge 20$ when attackers leave, $\Omega_{d{\rm tc}}$ decreases to $\omega_{\rm tc}$, as discussed in Remark 7 and Figure 5. However, under M_2, the performance constraint requirement in (CO4) is violated during the intervals $5 \le t \le 9$ and $t \ge 26$.

VI. Conclusion

In this work, we proposed a cooperative control framework for a team of agents to cooperatively track a target, in the presence of multiple physical attackers. Multiple safety and performance constraint requirements are taken into consideration. Specifically, on the one hand, to ensure safety we require that agents keep a safe distance from attackers and the target, which are formulated as constant constraint requirements. On the other hand, due to the presence of intelligent physical attackers, safety constraint requirements on inter-agent distances and performance constraint requirements on formation tracking are *environment-aware and dynamic*, which depend on distances between agents and physical attackers to ensure adequate adaptation of constraints in the presence of physical attackers. Neural network-based adaptive learning laws are incorporated to handle unknown target and attacker velocities. We show that formation tracking errors for the agents are both uniformly ultimately bounded, while all safety and performance constraints can be met. For future research we will explore tracking and capturing of multiple targets, and take cyber attacks into consideration.

Appendix

A. Agent and Attacker Set Radii

First, define

$$\bar{q}_m(t) \triangleq \text{softmax}_{\rho_{\rm u}}(e_m^{\rm T} q_1(t), \cdots, e_m^{\rm T} q_{N_{\rm u}}(t)),$$
$$\underline{q}_m(t) \triangleq \text{softmin}_{\rho_{\rm u}}(e_m^{\rm T} q_1(t), \cdots, e_m^{\rm T} q_{N_{\rm u}}(t)), \tag{31}$$
$$\bar{q}_{{\rm a}m}(t) \triangleq \text{softmax}_{\rho_{\rm a}}(e_m^{\rm T} q_{\rm a1}(t), \cdots, e_m^{\rm T} q_{{\rm a}N_{\rm a}}(t)),$$
$$\underline{q}_{{\rm a}m}(t) \triangleq \text{softmin}_{\rho_{\rm a}}(e_m^{\rm T} q_{\rm a1}(t), \cdots, e_m^{\rm T} q_{{\rm a}N_{\rm a}}(t)), \tag{32}$$

where $e_m \in \mathbb{R}^3$ ($m = 1, 2, 3$) is the mth column vector of identity matrix I_3, and $\rho_{\rm u} > 0$ and $\rho_{\rm a} > 0$ are introduced in Lemma 2.

As illustrated in Figure 3, for $t \ge 0$ agent and attacker sets are defined as

$$\mathcal{B}_{\rm u}(t) \triangleq \left\{\zeta \in \mathbb{R}^3 \middle| \|\zeta - q_{\rm u}(t)\| \le R_{\rm u}(t)\right\}, \tag{33}$$
$$\mathcal{B}_{\rm a}(t) \triangleq \left\{\zeta \in \mathbb{R}^3 \middle| \|\zeta - q_{\rm a}(t)\| \le R_{\rm a}(t)\right\}, \tag{34}$$

where centers and radii of agent and attacker sets are given as

$$q_{\rm u}(t) \triangleq \frac{1}{2}[\bar{q}_1(t) + \underline{q}_1(t),\ \bar{q}_2(t) + \underline{q}_2(t),\ \bar{q}_3(t) + \underline{q}_3(t)]^{\rm T}, \tag{35}$$

$$R_{\rm u}(t) \triangleq \frac{1}{2}\sqrt{\sum_{m=1}^{3}(\bar{q}_m(t) - \underline{q}_m(t))^2}, \tag{36}$$

$$q_{\rm a}(t) \triangleq \frac{1}{2}[\bar{q}_{\rm a1}(t) + \underline{q}_{\rm a1}(t),\ \bar{q}_{\rm a2}(t) + \underline{q}_{\rm a2}(t),\ \bar{q}_{\rm a3}(t) + \underline{q}_{\rm a3}(t)]^{\rm T}, \tag{37}$$

$$R_{\rm a}(t) \triangleq \frac{1}{2}\sqrt{\sum_{m=1}^{3}(\bar{q}_{{\rm a}m}(t) - \underline{q}_{{\rm a}m}(t))^2}. \tag{38}$$

B. Proof of Proposition 1

Proof: The target tracking error $\|q_{\rm c} - q_{\rm t}\|$ satisfies the following inequality

$$\begin{aligned}\|q_{\rm c} - q_{\rm t}\| &= \|q_{\rm c} - q_{\rm a} - q_{\rm t} + q_{\rm a}\| \ge \|q_{\rm c} - q_{\rm a}\| - \|q_{\rm t} - q_{\rm a}\| \\ &= \|q_{\rm c} - q_{\rm u} + q_{\rm u} - q_{\rm a}\| - \|q_{\rm t} - q_{\rm a}\| \\ &\ge \|q_{\rm u} - q_{\rm a}\| - \|q_{\rm c} - q_{\rm u}\| - \|q_{\rm t} - q_{\rm a}\|. \end{aligned} \tag{39}$$

For the first term in (39), since (CO1) is met, we have

$$\|q_{\rm u} - q_{\rm a}\| > R_{\rm a} + R_{\rm u} + \Omega_{\rm a}. \tag{40}$$

For the second term in (39), according to the definitions of $\bar{q}_m$ and $\underline{q}_m$ ($m = 1, 2, 3$) in (31), we can get

$$\begin{aligned}\underline{q}_m &= \frac{1}{N_{\rm u}}\sum_{i=1}^{N_{\rm u}} \underline{q}_m \le \frac{1}{N_{\rm u}}\sum_{i=1}^{N_{\rm u}} e_m^{\rm T} q_i = e_m^{\rm T} q_{\rm c} \\ &\le \frac{1}{N_{\rm u}}\sum_{i=1}^{N_{\rm u}} \bar{q}_m = \bar{q}_m,\end{aligned}$$

therefore, according to the definition of q_u in (35), $-\frac{1}{2}(\bar{q}_m - \underline{q}_m) \le e_m^T q_c - e_m^T q_u \le \frac{1}{2}(\bar{q}_m - \underline{q}_m)$. Now, recall the definition of R_u in (36), the term $-\|q_c - q_u\|$ in (39) can be expressed as

$$-\|q_c - q_u\| \ge -\frac{1}{2}\sqrt{\sum_{m=1}^{3}(\bar{q}_m - \underline{q}_m)^2} = -R_u. \tag{41}$$

Finally, we can take inequalities (40) and (41) into (39) to obtain $\|q_t - q_c\| > R_a + \Omega_a - \|q_t - q_a\|$. ■

ACKNOWLEDGMENT

The authors appreciate the Associate Editor and all Reviewers from IEEE TRANSACTIONS ON AUTOMATION SCIENCE AND ENGINEERING for the helpful comments and constructive suggestions during the review process.

REFERENCES

[1] L. Zhou, S. Leng, Q. Wang, Y. Ming, and Q. Liu, "Tiered digital twin-assisted cooperative multiple targets tracking," *IEEE Trans. Wireless Commun.*, vol. 23, no. 4, pp. 3749–3762, Apr. 2024.

[2] J. Gu, T. Su, Q. Wang, X. Du, and M. Guizani, "Multiple moving targets surveillance based on a cooperative network for multi-UAV," *IEEE Commun. Mag.*, vol. 56, no. 4, pp. 82–89, Apr. 2018.

[3] A. Albert and L. Imsland, "Survey: Mobile sensor networks for target searching and tracking," *Cyber-Phys. Syst.*, vol. 4, no. 2, pp. 57–98, Apr. 2018.

[4] F. Morbidi and G. L. Mariottini, "Active target tracking and cooperative localization for teams of aerial vehicles," *IEEE Trans. Control Syst. Technol.*, vol. 21, no. 5, pp. 1694–1707, Sep. 2013.

[5] L. Ma and N. Hovakimyan, "Vision-based cyclic pursuit for cooperative target tracking," *J. Guid., Control, Dyn.*, vol. 36, no. 2, pp. 617–622, Mar. 2013.

[6] H. Yu, K. Meier, M. Argyle, and R. W. Beard, "Cooperative path planning for target tracking in urban environments using unmanned air and ground vehicles," *IEEE/ASME Trans. Mechatronics*, vol. 20, no. 2, pp. 541–552, Apr. 2015.

[7] L. Briñón-Arranz, A. Seuret, and A. Pascoal, "Circular formation control for cooperative target tracking with limited information," *J. Franklin Inst.*, vol. 356, no. 4, pp. 1771–1788, Mar. 2019.

[8] P. Wieland and F. Allgöwer, "Constructive safety using control barrier functions," *IFAC Proc. Volumes*, vol. 40, no. 12, pp. 462–467, 2007.

[9] X. Xu, P. Tabuada, J. W. Grizzle, and A. D. Ames, "Robustness of control barrier functions for safety critical control," *IFAC-PapersOnLine*, vol. 48, no. 27, pp. 54–61, 2015.

[10] A. D. Ames, X. Xu, J. W. Grizzle, and P. Tabuada, "Control barrier function based quadratic programs for safety critical systems," *IEEE Trans. Autom. Control*, vol. 62, no. 8, pp. 3861–3876, Aug. 2017.

[11] M. Jankovic, M. Santillo, and Y. Wang, "Multiagent systems with CBF-based controllers: Collision avoidance and liveness from instability," *IEEE Trans. Control Syst. Technol.*, vol. 32, no. 2, pp. 705–712, Mar. 2024.

[12] K. P. Tee, S. S. Ge, and E. H. Tay, "Barrier Lyapunov functions for the control of output-constrained nonlinear systems," *Automatica*, vol. 45, no. 4, pp. 918–927, Apr. 2009.

[13] B. Ren, S. S. Ge, K. P. Tee, and T. H. Lee, "Adaptive neural control for output feedback nonlinear systems using a barrier Lyapunov function," *IEEE Trans. Neural Netw.*, vol. 21, no. 8, pp. 1339–1345, Aug. 2010.

[14] K. P. Tee and S. S. Ge, "Control of nonlinear systems with partial state constraints using a barrier Lyapunov function," *Int. J. Control*, vol. 84, no. 12, pp. 2008–2023, Dec. 2011.

[15] Q. Quan, R. Fu, M. Li, D. Wei, Y. Gao, and K.-Y. Cai, "Practical distributed control for VTOL UAVs to pass a virtual tube," *IEEE Trans. Intell. Vehicles*, vol. 7, no. 2, pp. 342–353, Jun. 2022.

[16] D. Q. Mayne, J. B. Rawlings, C. V. Rao, and P. O. M. Scokaert, "Constrained model predictive control: Stability and optimality," *Automatica*, vol. 36, no. 6, pp. 789–814, Jun. 2000.

[17] S. L. de Oliveira Kothare and M. Morari, "Contractive model predictive control for constrained nonlinear systems," *IEEE Trans. Autom. Control*, vol. 45, no. 6, pp. 1053–1071, Jun. 2000.

[18] X.-B. Hu and W.-H. Chen, "Model predictive control for constrained systems with uncertain state-delays," *Int. J. Robust Nonlinear Control*, vol. 14, no. 17, pp. 1421–1432, 2004.

[19] D. Q. Mayne, M. M. Seron, and S. V. Raković, "Robust model predictive control of constrained linear systems with bounded disturbances," *Automatica*, vol. 41, no. 2, pp. 219–224, 2004.

[20] M. Nezami, N. T. Nguyen, G. Männel, R. Kensbock, H. S. Abbas, and G. Schildbach, "Safe control architecture via model predictive control," *IEEE Trans. Control Syst. Technol.*, vol. 33, no. 4, pp. 1207–1220, Jul. 2024, doi: 10.1109/TCST.2024.3461173.

[21] S. Zhao, J. Zheng, K. Liu, J. Liu, and X. Wang, "Cooperative moving target fencing control for two-layer UAVs with relative measurements," *IEEE Trans. Autom. Sci. Eng.*, vol. 22, pp. 7145–7158, 2025.

[22] R. Ringbäck, J. Wei, E. S. Erstorp, J. Kuttenkeuler, T. A. Johansen, and K. H. Johansson, "Multi-agent formation tracking for autonomous surface vehicles," *IEEE Trans. Control Syst. Technol.*, vol. 29, no. 6, pp. 2287–2298, Nov. 2021.

[23] L. Kou, Z. Chen, and J. Xiang, "Cooperative fencing control of multiple vehicles for a moving target with an unknown velocity," *IEEE Trans. Autom. Control*, vol. 67, no. 2, pp. 1008–1015, Feb. 2022.

[24] K. Lu, S.-L. Dai, and X. Jin, "Cooperative constrained enclosing control of multirobot systems in obstacle environments," *IEEE Trans. Control Netw. Syst.*, vol. 11, no. 2, pp. 718–730, Jun. 2024.

[25] F. Huang, X. Chen, and Z. Chen, "Cooperative target enclosing control for multiple unmanned surface vehicles with unknown dynamics and safety assurance," *IEEE Trans. Intell. Vehicles*, vol. 10, no. 3, pp. 1678–1692, Mar. 2024, doi: 10.1109/TIV.2024.3431949.

[26] I. J. Gordon and H. H. Prins, *The Ecology of Browsing and Grazing*. Cham, Switzerland: Springer, 2008.

[27] L. Ma, Y.-L. Wang, and Q.-L. Han, "Cooperative target tracking of multiple autonomous surface vehicles under switching interaction topologies," *IEEE/CAA J. Autom. Sinica*, vol. 10, no. 3, pp. 673–684, Mar. 2023.

[28] A. J. Taylor and A. D. Ames, "Adaptive safety with control barrier functions," in *Proc. IEEE Amer. Control Conf.*, Jul. 2020, pp. 1399–1405.

[29] B. T. Lopez, J.-J.-E. Slotine, and J. P. How, "Robust adaptive control barrier functions: An adaptive and data-driven approach to safety," *IEEE Control Syst. Lett.*, vol. 5, no. 3, pp. 1031–1036, Jul. 2021.

[30] A. Isaly, O. S. Patil, R. G. Sanfelice, and W. E. Dixon, "Adaptive safety with multiple barrier functions using integral concurrent learning," in *Proc. IEEE Amer. Control Conf.*, 2021, pp. 3719–3724.

[31] M. Maghenem, A. J. Taylor, A. D. Ames, and R. G. Sanfelice, "Adaptive safety using control barrier functions and hybrid adaptation," in *Proc. Amer. Control Conf. (ACC)*, May 2021, pp. 2418–2423.

[32] R. Vidal, S. Rashid, C. Sharp, O. Shakernia, J. Kim, and S. Sastry, "Pursuit-evasion games with unmanned ground and aerial vehicles," in *Proc. IEEE Int. Conf. Robot. Autom.*, May 2001, pp. 2948–2955.

[33] R. Vidal, O. Shakernia, H. J. Kim, D. H. Shim, and S. Sastry, "Probabilistic pursuit-evasion games: Theory, implementation, and experimental evaluation," *IEEE Trans. Robot. Autom.*, vol. 18, no. 5, pp. 662–669, Oct. 2002.

[34] A. Antoniades, H. J. Kim, and S. Sastry, "Pursuit-evasion strategies for teams of multiple agents with incomplete information," in *Proc. 42nd IEEE Int. Conf. Decis. Control*, Dec. 2003, pp. 756–761.

[35] X. Sun and C. G. Cassandras, "Optimal dynamic formation control of multi-agent systems in environments with obstacles," in *Proc. 54th IEEE Conf. Decis. Control (CDC)*, Dec. 2015, pp. 2359–2364.

[36] J. Tordesillas and J. P. How, "MADER: Trajectory planner in multiagent and dynamic environments," *IEEE Trans. Robot.*, vol. 38, no. 1, pp. 463–476, Feb. 2022.

[37] C. Toumieh and A. Lambert, "Decentralized multi-agent planning using model predictive control and time-aware safe corridors," *IEEE Robot. Autom. Lett.*, vol. 7, no. 4, pp. 11110–11117, Oct. 2022.

[38] D. Panagou, D. M. Stipanovic, and P. G. Voulgaris, "Distributed coordination control for multi-robot networks using Lyapunov-like barrier functions," *IEEE Trans. Autom. Control*, vol. 61, no. 3, pp. 617–632, Mar. 2016.

[39] M. C. P. Santos, C. D. Rosales, M. Sarcinelli-Filho, and R. Carelli, "A novel null-space-based UAV trajectory tracking controller with collision avoidance," *IEEE/ASME Trans. Mechatronics*, vol. 22, no. 6, pp. 2543–2553, Dec. 2017.

[40] L. Zhang and G.-H. Yang, "Secure adaptive trajectory tracking control for nonlinear robot systems under multiple dynamic obstacles: Safety barrier certificates," *IEEE Trans. Ind. Electron.*, vol. 69, no. 11, pp. 11549–11559, Nov. 2022.

[41] P. Akella and A. D. Ames, "A barrier-based scenario approach to verifying safety-critical systems," *IEEE Robot. Autom. Lett.*, vol. 7, no. 4, pp. 11062–11069, Oct. 2022.
[42] D. Bernstein, *Matrix Mathematics: Theory, Facts, and Formulas*. Princeton, NJ, USA: Princeton Univ. Press, 2003.
[43] Y. V. Pant, H. Abbas, and R. Mangharam, "Smooth operator: Control using the smooth robustness of temporal logic," in *Proc. IEEE Conf. Control Technol. Appl. (CCTA)*, Aug. 2017, pp. 1235–1240.
[44] Y. Gilpin, V. Kurtz, and H. Lin, "A smooth robustness measure of signal temporal logic for symbolic control," *IEEE Control Syst. Lett.*, vol. 5, no. 1, pp. 241–246, Jan. 2021.
[45] P. Rabiee and J. B. Hoagg, "Soft-minimum and soft-maximum barrier functions for safety with actuation constraints," *Automatica*, vol. 171, Jan. 2025, Art. no. 111921.
[46] W. Xie, W. Zhang, and C. Silvestre, "Saturated backstepping-based tracking control of a quadrotor with uncertain vehicle parameters and external disturbances," *IEEE Control Syst. Lett.*, vol. 6, pp. 1634–1639, 2022.
[47] Z. Zuo and C. Wang, "Adaptive trajectory tracking control of output constrained multi-rotors systems," *IET Control Theory Appl.*, vol. 8, no. 13, pp. 1163–1174, Sep. 2014.
[48] A. Colombo and D. Del Vecchio, "Least restrictive supervisors for intersection collision avoidance: A scheduling approach," *IEEE Trans. Autom. Control*, vol. 60, no. 6, pp. 1515–1527, Jun. 2015.
[49] J.-H. Li, "Path tracking of underactuated ships with general form of dynamics," *Int. J. Control*, vol. 89, no. 3, pp. 506–517, Mar. 2016.
[50] Y. Wang, D. Wang, and S. Zhu, "Cooperative moving path following for multiple fixed-wing unmanned aerial vehicles with speed constraints," *Automatica*, vol. 100, pp. 82–89, Feb. 2019.
[51] I. Karafyllis, D. Theodosis, and M. Papageorgiou, "Forward completeness in open sets and applications to control of automated vehicles," *IEEE Trans. Autom. Control*, vol. 70, no. 4, pp. 2406–2421, Apr. 2025.
[52] C. H. Brighton and G. K. Taylor, "Hawks steer attacks using a guidance system tuned for close pursuit of erratically manoeuvring targets," *Nature Commun.*, vol. 10, no. 1, p. 2462, Jun. 2019.
[53] T. Ibuki, S. Wilson, A. D. Ames, and M. Egerstedt, "Distributed collision-free motion coordination on a sphere: A conic control barrier function approach," *IEEE Control Syst. Lett.*, vol. 4, no. 4, pp. 976–981, Oct. 2020.
[54] Y. Chen, A. Singletary, and A. D. Ames, "Guaranteed obstacle avoidance for multi-robot operations with limited actuation: A control barrier function approach," *IEEE Control Syst. Lett.*, vol. 5, no. 1, pp. 127–132, Jan. 2021.
[55] C. Peng, X. Liu, and J. Ma, "Design of safe optimal guidance with obstacle avoidance using control barrier function-based actor–critic reinforcement learning," *IEEE Trans. Syst., Man, Cybern., Syst.*, vol. 53, no. 11, pp. 6861–6873, Nov. 2023.
[56] F. Mehdifar, C. P. Bechlioulis, F. Hashemzadeh, and M. Baradarannia, "Prescribed performance distance-based formation control of multi-agent systems," *Automatica*, vol. 119, Sep. 2020, Art. no. 109086.
[57] R. Babazadeh and R. R. Selmic, "Directed distance-based formation control of nonlinear heterogeneous agents in 3-D space," *IEEE Trans. Aerosp. Electron. Syst.*, vol. 59, no. 3, pp. 3405–3415, Jun. 2023.
[58] M. Charitidou and D. V. Dimarogonas, "Virtual leader and distance-based formation control with funnel constraints," *IEEE Trans. Control Netw. Syst.*, vol. 12, no. 2, pp. 1342–1353, Jun. 2025, doi: 10.1109/TCNS.2024.3516559.
[59] A. G. Bors and I. Pitas, "Median radial basis function neural network," *IEEE Trans. Neural Netw.*, vol. 7, no. 6, pp. 1351–1364, Nov. 1996.
[60] S. Haykin, *Neural Networks: A Comprehensive Foundation*, 2nd ed., Upper Saddle River, NJ, USA: Prentice-Hall, 1998.
[61] R. J. Schilling, J. J. Carroll, and A. F. Al-Ajlouni, "Approximation of nonlinear systems with radial basis function neural networks," *IEEE Trans. Neural Netw.*, vol. 12, no. 1, pp. 1–15, Jan. 2001.
[62] Y. Li, S. Qiang, X. Zhuang, and O. Kaynak, "Robust and adaptive backstepping control for nonlinear systems using RBF neural networks," *IEEE Trans. Neural Netw.*, vol. 15, no. 3, pp. 693–701, May 2004.
[63] J. Ma, S. S. Ge, Z. Zheng, and D. Hu, "Adaptive NN control of a class of nonlinear systems with asymmetric saturation actuators," *IEEE Trans. Neural Netw. Learn. Syst.*, vol. 26, no. 7, pp. 1532–1538, Jul. 2015.
[64] J. Wei, Y.-J. Liu, H. Chen, and L. Liu, "Adaptive neural control of connected vehicular platoons with actuator faults and constraints," *IEEE Trans. Intell. Vehicles*, vol. 8, no. 6, pp. 3647–3656, Jun. 2023.
[65] Y. Li, S. Dong, K. Li, and S. Tong, "Fuzzy adaptive fault tolerant time-varying formation control for nonholonomic multirobot systems with range constraints," *IEEE Trans. Intell. Vehicles*, vol. 8, no. 6, pp. 3668–3679, Jun. 2023.
[66] K. D. Do, Z. P. Jiang, and J. Pan, "Robust adaptive path following of underactuated ships," *Automatica*, vol. 40, no. 6, pp. 929–944, Jun. 2004.
[67] X. Jin, "Fault-tolerant iterative learning control for mobile robots non-repetitive trajectory tracking with output constraints," *Automatica*, vol. 94, pp. 63–71, Aug. 2018.
[68] S.-L. Dai, S. He, M. Wang, and C. Yuan, "Adaptive neural control of underactuated surface vessels with prescribed performance guarantees," *IEEE Trans. Neural Netw. Learn. Syst.*, vol. 30, no. 12, pp. 3686–3698, Dec. 2019.
[69] X. Jin, "Adaptive fixed-time control for MIMO nonlinear systems with asymmetric output constraints using universal barrier functions," *IEEE Trans. Autom. Control*, vol. 64, no. 7, pp. 3046–3053, Jul. 2019.

Zhongjun Hu received the B.Eng. degree in automation from the College of Information Engineering, Zhejiang University of Technology, Hangzhou, China, in 2018, and the M.S. degree in electrical and computer engineering from The Ohio State University, Columbus, OH, USA, in 2020. He is currently pursuing the Ph.D. degree with the Department of Mechanical and Aerospace Engineering, University of Kentucky, Lexington, KY, USA.

His research interests include adaptive control and its application of multi-agent systems.

Jesse B. Hoagg (Senior Member, IEEE) received the B.S.E. degree in civil and environmental engineering from Duke University in 2002, and the M.S.E. degree in aerospace engineering, the M.S. degree in mathematics, and the Ph.D. degree in aerospace engineering from the University of Michigan in 2003, 2005, and 2006, respectively. He is currently the Donald and Gertrude Lester Professor and the Department Chair of Mechanical and Aerospace Engineering with the University of Kentucky.

Xu Jin (Senior Member, IEEE) received the Bachelor of Engineering (B.Eng.) degree (Hons.) in electrical and computer engineering from the National University of Singapore, Singapore, the Master of Applied Science (M.A.Sc.) degree in electrical and computer engineering from the University of Toronto, Toronto, ON, Canada, and the Master of Science (M.S.) degree in mathematics and the Doctor of Philosophy (Ph.D.) degree in aerospace engineering from Georgia Institute of Technology, Atlanta, GA, USA.

He is currently an Assistant Professor with the Department of Mechanical and Aerospace Engineering, University of Kentucky, Lexington, KY, USA. His current research interests include adaptive and iterative learning control with applications to intelligent vehicles, autonomous robots, and nonlinear multiagent systems. He was a recipient of the NSF CAREER Award in 2024 and was awarded the University of Kentucky Allan and Ginger Brown Aerospace Faculty Fellowship.